University of Alberta

T4 BACTERIOPHAGE FUNCTIONALIZED MICRO-CANTILEVERS FOR HIGHLY SPECIFIC BACTERIAL DETECTION

by

Luc Gervais

A thesis submitted to the Faculty of Graduate Studies and Research in partial fulfillment of the requirements for the degree of **Master of Science**

Department of Electrical and Computer Engineering

Edmonton, Alberta
Fall 2007

Your file Votre référence
ISBN: 978-0-494-33246-7
Our file Notre référence
ISBN: 978-0-494-33246-7

Try not. Do, or do not. There is no try. – Jedi Master Yoda

I dedicate this thesis to my parents: André and Nancy, and brothers: Patrick, Gabriel and Raphaël without whose love, support, discussions and sometimes arguments I would not have been able to become the person I am today.

Abstract

Bacteriophage are viruses that recognize bacteria more specifically than antibodies, and thus are extremely promising as highly-specific recognition elements for bacterial sensors.

A first streptavidin-immobilization chemistry immobilized genetically biotinylated T4 bacteriophage and minimized non-specific binding resulting in 5-10 phage/μm^2; a five-fold increase over simple physisorption. An ECIS device was employed to show the effect of a phage terminated surface on the growth of host bacteria.

A second T4 phage functionalization chemistry further minimized non-specific binding. Specific bacterial adsorption occurred at 55 cells/100μm^2. Non-specific binding of three *E. coli* strains not lysed by T4B occurred at 1 cell/100μm^2.

Cantilevers functionalized with T4 phage were resonated to detect the target *EC12 E. coli*. The frequency shift was confirmed by SEM image, showing abundant specifically bound *EC12*. Negative controls with non-specifically bound *6M1N1 E. coli*, and functionalized cantilevers without immobilized T4B with *EC12* showed an order of magnitude less resonance shift.

Acknowledgements

First of all, I would like to extend my thanks to my supervisor Dr. Stéphane Evoy. Thank you for believing in my ability to learn biology and to work in bioMEMS development. Without your patience, many meaningful discussions and insight none of this would have been possible. I am very grateful of the time and effort you have expended to train me. I will be taking this knowledge and experience with me in all my future endeavors. Thanks to Dr. Murat Gel for coaching me and teaching me much of what I know about nanoscience.

Dr. Béatrice Allain and the staff at Biophage Pharma inc. in Montréal, were very helpful with instructing me how to make phages and bacteria and taught me to be meticulous when dealing with biology. Thanks a lot for mentoring me with microbiology techniques and for making the Electrical Cell Impedance Sensing (ECIS) experiments possible.

Thanks to Feng Wang, Megan Brebber at the National Institute for Nanotechnology (NINT) for helping me with biochemistry and showing me that sometimes there was a better protocol then the one I came up with on my own. Thanks a lot to Daniel Salomon for his patience with all my Scanning Electron Microscopy (SEM) questions.

Special thanks go to the staff at the University of Alberta NanoFab: Dr. Ken Westra, Kristian Olsen, Les Schowalter, Scott Munro and Stephanie Bozic. Thanks for making my adaptation to fab work a pleasant one, for training me on the multitude of equipment and for making sure I didn't lose a finger in the Piranha cleaning, HF or KOH etching. Thanks very much to Lee Fischer for his patience and answers to my many microfabrication and cantilever questions.

I would like to thank Lee Fischer, Andrew Murray, Erik Luber and Shufen Tsoi for their comforting conversations and friendship.

Table of Contents

List of Tables

List of Figures

List of Abbreviations

AFM	Atomic force microscope
bioMEMS	Biological Micro-ElectroMechanical Systems
BSA	Bovine serum albumin
BBSA	Biotinylated bovine serum albumin
CCD	Charge-coupled device
cfu	colony forming unit
CMOS	Complementary metal-oxide semiconductor transistors
dsDNA	Double stranded deoxyribonucleic acid
ECIS	Electrical cell impedance sensing
ELISA	Enzyme-linked immunosorbent assay
FITC	Fluorescein isothiocyanate
kbps	nucleic acid kilo base pairs
kDa	kilo Dalton
LB	Luria-Bertani media

PBS	Phosphate buffered saline
PBST	Phosphate buffered saline tween
PCR	Polymerase chain reaction
pfu	phage forming unit
QCM	Quartz crystal microbalance
SA	Streptavidin
SAM	Self-assembled monolayer
SEM	Scanning electron microscopy
SiNW	Silicon nanowires
ssDNA	Single stranded deoxyribonucleic acid
SPR	Surface plasmon resonance
T4B	Genetically biotinylated T4 bacteriophage
TRITC	Tetramethylrhodamine isothiocyanate
TSB	Tryptic soy broth
UV	Ultraviolet light

1

BioMEMS for Pathogen Detection

Microorganisms such as bacteria and viruses are commonly found in the environment. They are present in soil, contaminated water, raw vegetables, raw meats, and human secretions such as blood and saliva. Inside and outside of the human body alone there are over 500 kinds of bacteria [1].

Not all microorganisms are pathogenic. Many bacterial species exist in a symbiotic relationship with the host organism and cause no physiological harm. For example, there are many different strains of *E. coli* bacteria that are an essential part of the bacterial flora of the human intestinal tract and are crucial for digestion in the large intestine [1–4]. However, pathogenic strains of *E. coli* produce a powerful endotoxin that can cause pneumonia, meningitis and diarrhea among other potentially deadly illnesses [5, 6].

Microbial organisms are still the major cause of death in developing countries. In addition, many pathogenic organisms are potential biological warfare agents. For example, *bacillus anthracis* can cause anthrax, *salmonella typhi* can lead to thyphoid fever and *mycobacterium tuberculosis* can result in tuberculosis. Most humans are susceptible to infection by these microorganisms which have very high fatality rates.

The detection and identification of pathogens in food products, drinking water supplies and hospitals continue to rely mostly on conventional microbiological culture techniques.

These tests are based on assessing a bacterium's ability to grow in plates or tubes containing a variety of media (solid or liquid) under various conditions.

While detection of a small number of bacteria is possible by incubation, growth of bacteria to numbers sufficient for identification can take several days. In addition, further biochemical and serological tests are required to confirm the identity of the agent. Polymerase chain reaction (PCR) may also be used to amplify a small amount of genetic material from bacteria [7, 8]. Alternatively, bacterial identification using enzyme-linked immunosorbent assay (ELISA) is conducted by testing antibody-antigen interaction with the targeted bacterium and can be performed within a working day [9]. Combined PCR-ELISA increases sensitivity of the conventional PCR method by 100 to 1000 fold [10, 11]. However, these techniques still require an enrichment step during which bacteria are grown to the levels required for detection. In addition, problems associated with enzyme inhibition and DNA extraction have made direct detection of low numbers of bacteria in foods by PCR difficult to achieve.

Therefore, there has been sustained interest towards the development of biosensing systems that would circumvent the limitations of conventional techniques. A typical biosensor platform couples a physical transducer (electrochemical, mechanical, thermal, or optical) with a specific recognition probe such as an enzyme, nucleic acid, cell, antibody or artificial receptor. The interaction between the probe and the target is converted to a quantifiable signal by the transducer.

Diagnostic Biological Micro-Electromechanical Systems (bioMEMS) can be used to detect many possible biological analytes such as whole cells, proteins, viruses, DNA and small molecules. The rest of this chapter will review label-free bioMEMS technologies used for diagnostics and pathogen detection applications. There exists a wide variety of biosensor techniques that have been developed to sensitively detect biomolecules in real-time. Label-free biosensor systems that are under intense scientific investigation are first discussed. Surface Plasmon Resonance (SPR) and Quartz Crystal Microbalance (QCM) are reviewed. Electrical detection sensors are reviewed as well as cantilever based biosensors.

1.1 Surface Plasmon Resonance

Surface Plasmon Resonance is the basis of many biosensors and lab-on-a-chip sensors. The SPR technique measures the adsorption of particles to the surface of planar metal surfaces. The typical metal used in biosensors is gold because of its biocompatibility and ease of functionalization with thiol chemistries. However, metals such as silver, copper, titanium and chromium are also compatible with SPR.

A diagram of an SPR sensor is shown in figure 1.1. Laser light is totally reflected at the interface of an optically dense metal and less dense dielectric. An evanescent wave is generated that is amplified by resonance of conducting electrons (plasmons) in a thin metal layer of about 50nm. The surface plasmon electromagnetic wave occurs at the interface of the metal and the dielectric (vacuum, air, water) and travels parallel to the metal/dielectric boundary. Some photons from the incoming light are absorbed and converted to surface plasmons. These photons are not reflected, causing a shadow in the reflected light that is detected at a photodiode array. A change in the refractive index at the metal/dielectric boundary caused by the adsorption of molecules to the metal causes shifts in the resonance angle. This allows for real-time label-free measurements of biomolecule binding.

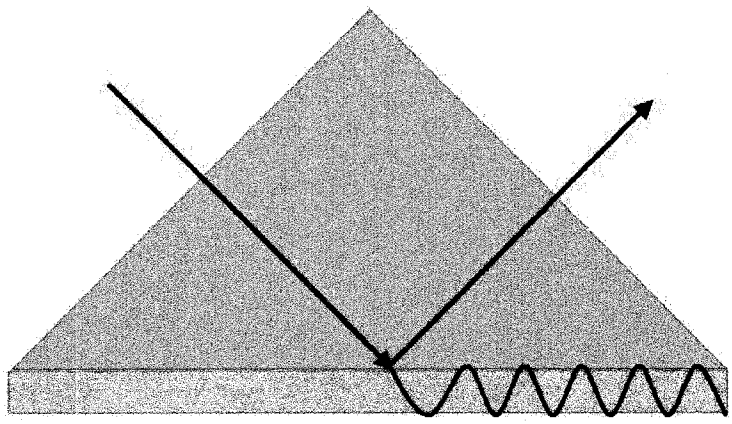

Figure 1.1: Surface plasmon resonance detection scheme

The SPR technique has been used to detect DNA-DNA interactions and protein binding such as antibody-antigen interactions. The commercially available BIACORE SPR sensor [12] (Pharmacia, Sweden) can be used to measure receptor-ligand interactions in real-

time. Biological probe molecules are immobilized onto a dextran matrix covering a gold transducer surface. A fluid flow system is used to introduce oligonucleotides and induce hybridization and measurable signals within a few minutes at room temperature. The IAsys system (Affinity Sensor, UK) is a similar SPR biosensor. The gold film is replaced by a titania(TiO_2) or hafnia(HfO_2) film that acts as a high refractive index resonant layer. A Dextrin or aminosilane monolayer is used to modify the sensor surface. Femtomolar detection of DNA hybridization has been achieved using this technique. Spreeta (Sensata Texas Instruments, US) is another commercially available SPR biosensor designed to be easily manufacturable in large quantities [13].

A variety of pathogens have been detected using SPR. Homola *et al.* have detected the pathogen staphylococcal enterotoxin B (SEB) in concentrations as low as 5 ng/mL in milk samples using an SPR biosensor [14]. The SPR technique has been used to detect whole cells. Oh *et al.* immobilized a self-assembled protein G layer onto a gold surface to detect *E. coli* with a detection limit of about 10^4 cells/mL [15]. The Spreeta biosensor was used with an antigen antibody coupling to the sensor surface to detect *E. coli* in a number of food products such as milk, apple juice and ground beef with a sensitivity of 10^3 cells/mL and shown to be specific to *O157 E. coli* when compared to *K12 E. coli* and *Shigella* bacteria [16].

The SPR technique depends on changes in refractive index and therefore can't differentiate between molecules with similar refractive indexes. For example, some lipoproteins, glycoproteins and nucleic acids have the same order of magnitude refractive indexes [17]. It is important therefore to be careful to choose sensor surface functionalizations that only allow the target analyte to bind, and exhibit minimal non-specific binding.

1.2 Quartz Crystal Microbalance

The Quartz Crystal Microbalance (QCM) operates by measuring the mass change that results in a shift in resonance frequency of a quartz crystal plate. A positive-feedback oscillator circuit is used to detect the quartz piezoelectric crystal's fundamental resonance frequency. As particles adsorb onto the surface, the small mass changes on the crystal surface causes the resonance frequency to decrease. Selectivity is dependent on the functionalization used for the sensor surface. Similar selectivity and sensitivity are exhibited by QCM and SPR sensors.

In general, the surface of a quartz crystal sensor is coated with a selective binding substance such as antibodies for bacteria, and then the solution containing the analyte is washed over the sensor. As bacteria bind to the sensor surface, mass will increase while the resonance frequency will decrease proportionally. Using this approach, QCM sensors were developed for *Vibro cholerae* [18], *Salmonella typhimurium* [19] and *L. monocytogenes* [20].

Ben-Dov *et al.* have developed a QCM sensor for *Chlamydia trachomatis* in urine samples by functionalizing the electrode with antibodies [21]. A primary cysteamine monolayer was assembled onto a gold electrode associated with the quartz crystal. The monolayer was then modified with anti-C antibody. The sensor was determined to have a bacteria detection limit of 260 ng/mL.

The QCM technique has several disadvantages. A relatively long incubation period is required to detect bacteria, many washing and drying steps are required and regenerating the crystal surface for subsequent measurements is non trivial. The performance of QCM degrades dramatically when the QCM is resonated in liquid as compared to air due to viscous damping. This makes it challenging to operate the resonators in an aqueous environments in which biologically relevant reactions occur. In addition, QCM is very sensitive to temperature change and thus precise control of the temperature of the chamber is required.

1.3 Electrochemical Detection Sensors

Electrochemical detection is common in many commercially available bioMEMS sensors due to its amenabity to miniaturization and portability. Figure 1.2 shows three fundamental electrochemical sensing techniques that are commonly used in micro and nano scale sensors. Conductometric biosensors measure the change in impedance causes by a change in the ions between the electrodes. Ampererometric biosensors measure the electrical current caused by electrons involved in redox biochemical reactions. Potentiometric biosensors probe the change in potential between electrodes caused by biochemical reactions or the presence of ions.

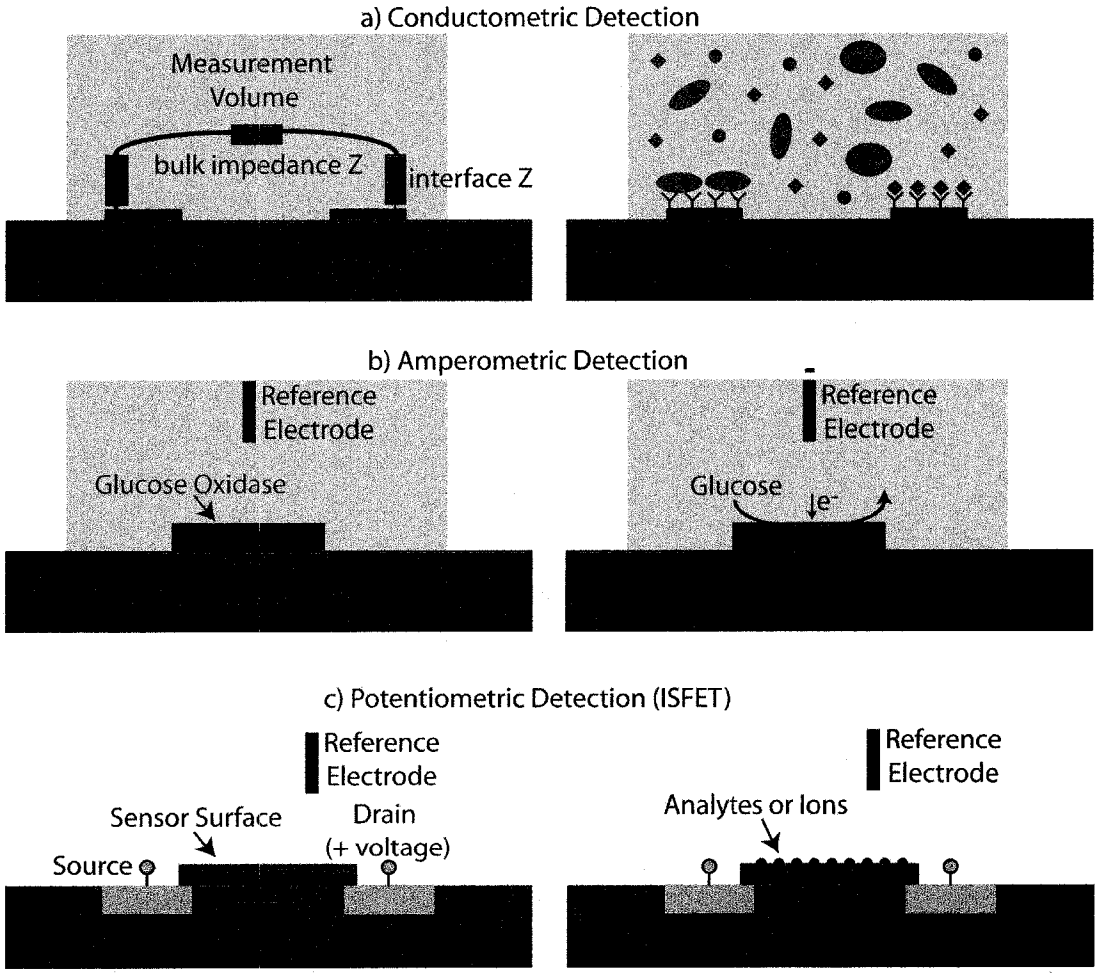

Figure 1.2: Electrochemical biosensor detection

1.3.1 Conductometric Biosensors

Conductometric sensors can be used to measure changes in impedance between two electrodes at the interface or in solution. Due to their simplicity and ease of use, conductance techniques have been successfully applied to measure protein reactions, antigen-antibody binding and DNA binding.

A sensor has been developed to study the excitatory or inhibitory electrical response of neurons to stimulation from electrical electrodes [22]. Neurons were cultured onto arrays of iridium electrodes and their electrical signals were measured after exposure to toxins and harmful chemicals.

Microfabricated sensors coupled with selective enzyme membranes provide information about ionic strength in electrolytes. They have been used to detect blood biochemicals such as glucose, urea, uric acid, creatine and creatinine [23–25]. Conductance and amperometric sensors were developed to detect organophosphate insecticides [26].

Sensors have been developed to detect DNA hybridization [27, 28]. A commercial application of electrical measurements of DNA hybridization has been developed [29, 30]. The hybridization of DNA is detected by measuring conductivitiy changes caused by the binding of oligonucleotides functionalized with gold nanoparticles.

The metabolic activity of microorganisms has been measured within micro-fluidic channels. Bacteria cells growing on electrodes within the channels were detected using impedance changes [31].

1.3.2 Amperometric Biosensors

The current generated by electrons involved in redox reactions are measured in amperometric biosensors. Typically the electron current of an enzyme-catalyzed redox reactions is measured at a working electrode. A good example of this is glucose sensors [32, 33]. Glucose oxidase immobilized on a carbon electrode converts glucose in solution to gluconic acid and hydrogen peroxide that is measured between two electrodes. These sensors measure the formation of hydrogen peroxide or the consumption of oxygen. Microfabricated sensors have been developed to take advantage of this effect. Working and reference electrodes are fabricated with an enzyme coating layer over the working

electrode. These devices have been used to detect glucose, lactose and urea [34–36].

Matrices of electroactive hydrogels have been used to physically entrap enzymes for detection of cholesterol and glucose [37, 38]. Amperometric biosensors have been used to detect lactate and human blood metabolites in single cell experiments [39].

The detection of DNA hybridization has been achieved by ferrocenyl derivatives integrated site-specificaly into DNA oligonucleotides [40, 41]. Fully electronic DNA detection has been achieved using the CMOS process and electrochemical redox cycling [42–44]. An active area of the transistor is patterned for DNA immobilization. The negative electric charge of DNA molecules modifies the drain current of the transistor. The hybridization of DNA results in a charge increase and a change in the measured output current. Analog to Digital converters and output circuitry are provided on chip.

1.3.3 Potentiometric Biosensors

Potentiometric sensors measure the potential difference between two electrodes. Ion-sensitive field effect transistors (ISFET) are a common type of potentiometric sensor. ISFETs have been used as pH sensors [45]. Human blood analytes have been detected on ISFETs with ion-selective ionophores immobilized onto polyvinyl chloride (PVC) [35]. A CMOS ISFTET that detects pH and oxygen partial pressure has been developed to measure cellular respiration and acidification [46].

Light-addressable potentiometric sensors (LAPs) are used to detect ions using a field emitting transistor FET and incoming light. Detection of oxygen and pH sensing for cell metabolism have been achieved using LAPs [47, 48]. Additionally, LAPs have been used to detect potassium, magnesium and calcium ions [49].

Detection of DNA has been achieved using micro-scale potentiometric sensors [50]. Silicon FETs were used to measure the surface charge increase of DNA hybridization on the sensor surface. Probe DNA was immobilized electrostatically on a positively charged poly-L-lysine layer. Nanomolar concentrations of DNA were detected and single base mismatches within 12-mer oligonucleotides were distinguished.

Nanometre scale potentiometric sensors have been been fabricated out of silicon nanowires and carbon nanotubes enhancing sensitivity due to higher surface to volume ratios.

Boron-doped silicon nanowires (SiNWs) have been fabricated by Cui *et al.* to concentration dependently detect biological and chemical species [51]. Amine and oxide functionalized SiNWs were used as pH sensors. Biotin functionalized SiNWs were used to detect streptavidin. Antigen functionalized SiNWs have shown detection and reversible binding of antibodies and the metabolic indicator Ca^{2+}. Besterman *et al.* have demonstrated that single-wall carbon nanotubes coated with the redox enzyme glucose oxidase can be used to measure changes in conductance upon changes in pH [52]. A single nanotube produced a steplike response upon the introduction of glucose oxidase.

1.4 Cantilever Based Sensors

Recently mechanical detection of biological entities has been accomplished using micro and nano-sized cantilevers. Cantilevers have been developed to transduce a variety of signals such as temperature, pH, mass, stress and electromagnetic field. The measurements provided by cantilevers have been demonstrated to be several orders of magnitude more sensitive than that of SPR and QCM [53–55].

1.4.1 Deflection and Resonant Cantilevers

Cantilevers sensors can operate in two modes: stress sensing or mass sensing. In stress sensing (Figure 1.3), differential surface stress is measured between opposite sides of the cantilever. A uniform stress acting on the material will result in either compressive stress or tensile stress. One side of the cantilever is functionalized to selectively perform a biochemical reaction and the other side is passivated. Adsorption induced stress is therefore only present on one side of the cantilever resulting in a bend with a constant radius of curvature.

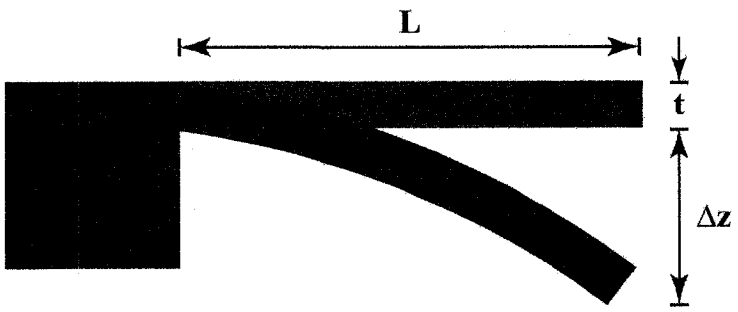

Figure 1.3: Surface stress detection using a deflecting cantilever

A rectangular beam of length L, thickness t is fixed at one end and free to move at the opposite end. The differential surface stress change and the resulting deflection Δz at the free end can be related as [56]:

$$\Delta z = 4(\frac{L}{t})^2 \frac{(1-v)}{E}(\Delta\sigma_1 - \Delta\sigma_2) \tag{1.1}$$

where E is Young's modulus, v is Poisson's ratio, $\Delta\sigma_1$ and $\Delta\sigma_2$ are the change in surface stress on the top surface of the cantilever and the bottom surface respectively. From the equation, it can be seen that stress sensitivity increases with the length to thickness ratio $\frac{L}{t}$. Therefore long and thin cantilevers are required to achieve high sensitivity, allowing more molecules to bind and cause a stress change. Stress sensitivity of the cantilever can also be increased by using a material with a lower Young's modulus, allowing the cantilever to bend more easily.

In mass sensing (Figure 1.4), the cantilever is excited mechanically to vibrate at its fundamental resonant frequency. Typically, ambient noise or a piezoelectric tube or disk are used. Once a biological entity binds to the cantilever, the resulting change in mass can be measured by detecting a resonant frequency shift.

A rectangular cantilever's fundamental resonant frequency f_0 can be calculated as [57]:

$$f_0 = \frac{1.875^2}{2\pi}\frac{t}{L^2}\sqrt{\frac{E}{12\rho}} \tag{1.2}$$

where ρ is the density of the cantilever's material. Given a constant thickness, shorter cantilevers are used to achieve higher frequencies with higher sensitivity and lower noise.

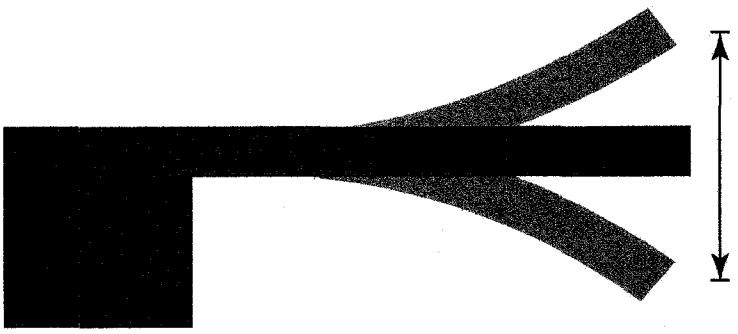

Figure 1.4: Mass change detection using a resonant cantilever

The cantilever's fundamental resonant frequency is affected by the viscocity of the medium surrounding the cantilever. A high viscocity medium will damp the cantilever and reduce the fundamental resonance frequency f_0 and the quality factor Q. For this reason, cantilever experiments requiring high sensitivity are typically conducted in high vacuum to allow higher resonant frequencies.

A change in mass Δm on a cantilever can be expressed as a function of a change in frequency [58]:

$$\Delta m = \frac{k}{4n\pi^2}\left(\frac{1}{f_1^2} - \frac{1}{f_0^2}\right) \tag{1.3}$$

where k is the spring constant of the cantilever, f_0 the unloaded resonant frequency before functionalization and f_1 the resonant frequency after mass addition. In the case where the mass is placed at the free end of the cantilever $n = 1$. In the case were a mass is uniformly loaded across the cantilever $n \approx 0.24$. During adsorption of biochemical species on the surface of a cantilever, mechanical properties such as the spring constant can also be changed by the deposited material. For example, the adsorption of water to a gelatin coated cantilever has been shown to increase resonance frequency, countering the mass increase effect [59, 60]. To minimize the coupling of the mass and stiffness changes, the sensing layer of the cantilever can be localized at the tip of the free end. Decreasing the mass of the cantilever and increasing the quality factor will result in better mass sensitivity.

The minimum detectable frequency change Δf_{min} can be determined as a function of the quality factor Q [58]:

$$\Delta f_{min} = \frac{1}{A}\sqrt{\frac{f_0 k_B T B}{2\pi k Q}} \tag{1.4}$$

where A is the root mean-squared amplitude of the cantilever beam, k_B is Boltzmann's constant, T is the temperature, f_0 is the natural resonant frequency, k is the spring constant and B is the measurement bandwidth. An increase in the quality factor Q and of oscillation amplitude A decreases the minimum detectable frequency shift. The latter can be achieved by externally driving the cantilever beam and thus increasing the amplitude or by operating the cantilever in vacuum.

1.4.2 Cantilever Deflection Detection Schemes

Their exists a number of methods to detect the deflection of cantilever beams with sub Angstrom resolution. Cantilever biosensors have been developed using optical and electrical detection schemes to obtain resonance or deflection measurements of cantilevers.

Optical Deflection Detection

The *beam bounce* or *optical lever* technique is shown in Figure 1.5. A low power laser diode emits visible light that is focused on the cantilever. The light bounces off the surface of the cantilever into a split photodiode detector. The reflected light moves on the photodetector proportionally to the cantilever deflection. Often a reflective layer of gold or aluminum is coated onto the cantilever to improve the signal. This is the method most commonly used in Atomic Force Microscopy (AFM). This method has low cost and is highly efficient. The size of the detectable cantilever is limited by the low power laser diode beam spot in the order of tens of micrometres. Therefore, this technique can only be used in micrometre sized cantilevers.

Another optical technique employs interference of light to obtain the displacement of the cantilever [61]. Interference occurs between a reference laser and a laser beam reflected off the cantilever. This is achieved by using the cleaved end of an optical fiber and bringing it close to the cantilever surface. The light is reflected internally at the interface between

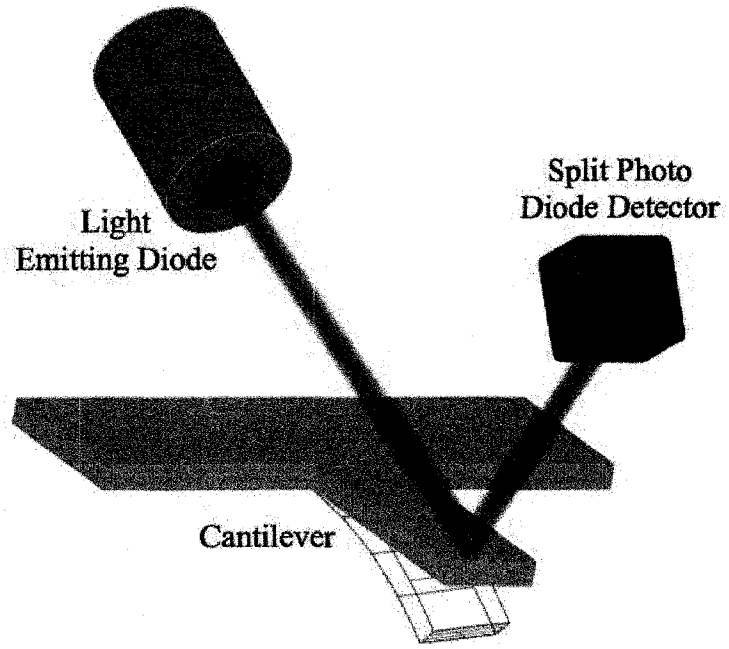

Figure 1.5: Beam bounce deflection detection of a cantilever

the fiber and the medium, and partly at the cantilever and back into the fiber. This results in a phase shift between the two reflected beams. This interference can be detected by a photodiode. Measurements of deflections in the range of 0.01 Å have been achieved [61]. The absolute deflection of the cantilever is defined within a single wavelength, thus this technique can only be used with very small nanometre sized cantilevers.

Electrical Deflection Detection

In capacitive sensing, a cantilever forms one of the parallel plates of a capacitor. As the distance changes, the capacitance changes. This method has been shown to be highly sensitive at measuring small absolute displacements of cantilevers [62]. However this method is unable to measure large displacements and does not work in electrolyte solutions because of Faraday currents between the capacitor plates. Therefore, this method is of limited use in biosensors.

Piezoresistive cantilevers are another option for on-chip detection. Piezoresistive materials, such as doped silicon, change electrical conductivity when they are under stress. Piezoresistive stress sensors are integrated into cantilevers with a Wheatstone bridge to

measure resistivity [63,64]. Until recently, piezoresistive cantilevers were crippled by their inability to be used in liquid environments because of Faraday currents that would short circuit the resistors. Thin and passivated resistors have been fabricated onto cantilevers that can be used in electrolyte solutions [65]. Alternatively, resistors and electrical wires are encapsulated in low-pressure chemical vapor deposition (LPCVD) silicon nitride [66].

Piezoresistive cantilevers are under intense development to increase resolution and lower noise. One of the main advantages over optical techniques is that the entire detection system can be integrated on chip without the need for laser alignment. Optical techniques can be affected by changes in the optical properties of the medium such as refractive index or opacity that would affect the position of the laser spot on the photodiode detector. Piezoresistive cantilevers are not subject to this problem and can essentially operate in an opaque medium if required. Additionaly, CMOS read-out circuits can be implemented onto the same chip as the cantilever sensor [67].

Resistors in piezoresistive cantilevers can be used to heat the surface of the cantilever. This has been proposed to be used to break ligand-receptor binding to regenerate the sensing layer of a biosensor [68]. This has also been proposed as a technique to monitor PCR reactions [69].

Piezoresistive cantilevers have recently been made from SU8 polymer [70]. SU8 is a chemically resistant polymer that is easier to work with than silicon and silicon nitride because it can be spun similarly to photoresist. The piezoresistor is fabricated out of gold. These cantilevers exhibit a lower spring constant and thus are more sensitive for deflection measurements.

1.4.3 Biosensing Applications

As mentioned before, cantilevers can be operated in both static bending mode or resonant frequency change mode. The bending of a cantilever is very sensitive to changes on the surface of the cantilever. This is very useful in detecting structural changes in chemically adsorbed layers on the cantilever surface. However, it is often the case that the chemical effects are not fully understood and therefore it is difficult to obtain quantitative measurements from the deflection of the cantilever. In addition, the bending of the

cantilever can be sensitive to temperature effects and other disturbances in the cantilever environment. Deflection is a good tool to detect uniform layers of small biological entities such as ions, proteins and DNA. Furthermore, detection can easily be carried out in the liquid environment of the biological reaction.

Measuring the resonance frequency change provides more quantifiable results since the mass change can easily be calculated. However, the measurement setup is more complicated since the cantilever needs to be driven and frequency feedback electronics are required which can add noise to the signal. Additionaly, frequency changes can be caused by temperature change or changes in the spring constant of the cantilever. Resonance is well suited for detecting larger biological entities that do not form a uniform layer such as virus particles and whole cells.

Deflection Detection

Using the deflection detection method, only one side of the cantilever must be functionalized and the other side must be passivated to block non-specific interaction. Thiol self assembled monolayers (SAMs) are commonly used on a deposited gold film on one side of the cantilever. In some cases, different thiols are used on both sides of the cantilever. On one side a thiol that will bind to the analyte is used, on the other side a thiol that prevents non-specific binding is used [68].

Thiol-modified cantilevers have been employed to detect changes in pH or salt concentration in liquid [68, 71]. Thiol modified cantilevers have been shown to have different pH dependencies when functionalized with Mercaptohexadecanoic acid and hexadecanethiol [72].

Hg^{2+} ions have been detected in trace quantities on gold-coated cantilevers [73]. Coating the surface of the cantilevers with ion-selective SAMs has enabled the detection of caesium and calcium ions [74]. Microcantilevers coated with hydrogels containing tetraalkylammonium salts were used to detects CrO_4^{2-} in liquid [75]. A plant metal binding protein, AgNt84-6, has been coated onto cantilever and used to detect heavy metal ions [76]. Organophosphorous compound nerve agents have been detected using a microcantilever coated with a bilayer of L-cysteine and Cu^{2+} [77].

The specific binding of proteins to cantilevers has been well characterized. Cantilever deflection has been observed as a result to antigens binding to an antibody coated microcantilever [78, 79]. Specific binding of two forms of the prostate specific antigen (PSA) has been detected over a range of concentrations [80]. The interaction of biotin and streptavidin and herbicide binding to its monoclonal antibody have been observed using static deflection cantilevers. [68, 81].

Cantilevers have being used in the field of genomics. Microcantilever sensors have been used to study the adsorption kinetics and mechanical properties of thiolized DNA on gold [82]. Arrays of deflecting cantilevers have been applied to detect DNA hybridization [83]. A single mismatch between two 12-mer oligonucleotides was detected in the hybridization of complimentary oligonucleotides. Hansen *et al.* have demonstrated similar results with a 10-mer oligonucleotide [84].

Resonating Detection

Resonant cantilever allow for quantifiable measurements of biological entities. However, measuring frequency changes in liquid is a problem that still needs to be solved. The high damping that results in liquids reduces the resonance frequency and the quality factor. Changing the medium from air to water typically results in a decrease of two orders of magnitude in quality factor. An increase in effective mass due to the added mass of the liquid displaced by the cantilever causes the damping. The frequency change associated with changing the medium from air to liquid has been used to quantify the density and viscocity of different liquids [85, 86].

Due to the inherent decrease in performance associated with resonating cantilevers in fluids, resonance measurements are usually carried out in vacuum or air after biological entities are introduced to bind on the cantilevers. Resonating cantilevers are well suited for detecting larger biological entities that do not result in continuous coverage of the cantilever surface, and thus do not result in a uniform stress change that can be measured using deflecting cantilevers.

Bacterial cells, such as *E. coli*, and antibodies have been detected using resonating cantilevers [57, 58]. *E. coli* specific antigens were immobilized onto the surface of

cantilevers and exposed to the bacterial or antibody solution. The cantilevers where then resonated in air and detected using the beam bounce technique. Vaccinia virus particles have also been detected similarly [87].

Polymer coated resonant cantilevers have been developed for mass sensing of volatile organic compounds such as n-octane and toluene [88]. CMOS transducers, driving and signal conditioning circuitry as well as the micro-cantilevers were fabricated on the same chip.

Piezoelectric resonating cantilevers have been used to measure antigen-antibody binding. Cantilevers fabricated out of $Pb(Zr_{0.52}Ti_{0.48})O_3$ (PZT) have been used to detect prostate-specific antigen and C-reactive protein [89, 90]. Nanocantilevers were fabricated from composite layers of Ta/Pt/PZT/Pt/SiO_2 on a SiN_x supporting layer for electrical electrical self-excitation and sensing. Specific antigens were immobilized using a Calixcrown SAM onto a deposited gold surface.

1.5 Future Direction of BioMEMS

Several label-free detection technologies have successfully been applied to MEMS biosensors. Biological analytes can be detected using a variety of methods and while they certainly all have their pros and cons, there currently is no detection scheme that is ubiquitous.

Regardless of what detection technique is used, often the development of these technologies as viable biosensing systems requires the use of a recognition probe offering high levels of specificity, selectivity, and stability. The biosensor will only be be as sensitive to the biological entity as the chosen recognition probe.

Biosensors have been developed with recognition probes such as immobilized enzymes, ions specific polymer matrices, nucleic acids and proteins. Antibodies are frequently used as recognition receptor systems for the specific detection of antigens. While antibodies may offer some degree of selectivity and speficity (especially monoclonal antibodies), they suffer from environmental instabilities and require arduous and cost-intensive methods for their production, isolation and purification. In addition, polyclonal antobodies are limited by their heterogenicity towards other species, strains or molecules. Thus, there is a need

for alternative probe selection.

Arguably much of the novelty of today's biosensors is attributed to original chemical functionalization schemes. In the following chapters we will explore the functionalization of bioMEMS using a novel alternative to antibodies, bacteriophage which are highly specific bacteria viruses.

2

Bacteriophage: Highly Specific Bacterial Recognition Probes

2.1 Introduction to Bacteriophage

Bacteriophage are bacteria-specific viruses and are the most abundant organisms on Earth. Coastal sea water typically contains 10^7 tailed phage particle per millimetre at the surface and the global population of phage is estimated to be greater than 10^{30}. The total number of phage exceeds bacterial cells by at least ten times [91, 92].

Every strain of bacteria has its own bacteriophage that can be isolated from the growth environment of the bacteria. Phages are present in drinking water, milk, fermented vegetables and meats, sewage, feces and soil among other places.

Since their independent discovery by Edward Twort (1915) and Felix d'Herelle (1917), bacteriophage have spurred interest as anti bacterial agents [93]. However, due to the subsequent discovery of antibiotics, bacteriophage therapy research was largely abandoned in western science. Nevertheless, bacteriophage therapy has been used and researched in France, the former Soviet Union and Georgia [94].

Antibiotic resistant bacteria has created a renewed interest in bacteriophage therapy resulting in intense research efforts to use these viruses to kill pathogenic organisms.

Recent research in the United States and Britain have confirmed results from eastern Europe [95–97].

When treated with the appropriate bacteriophage, protection of mice against systemic infections of *Pseudomonas* and *Acinetobacter* has been shown. As few as 100 phage were needed to protect against infection with over 100 million bacteria [98]. Phages have been used to treat infections of burn patients. Guinea pigs treated with phage against *Pseudomonas aeruginosa* bacteria have improved tolerance to skin-grafts [99].

A small number of phage have been studied in great detail. Some examples of phage whose genome have been sequenced and extensively characterized are λ [100], M13 [101], T4 [102], T7 [103] and f1 [104]. The vast body of knowledge and understanding of these phage systems allows for exciting applications in technologies such as phage display and biosensors that will be covered in this section.

2.1.1 Bacteriophage Structure and Composition

Bacteriophage exist in many different shapes and sizes but all share some common structural components. A T4 phage is shown in Figure 2.1. It is about 200 nm in length and 90 nm wide. Bacteriophage typically range between 24 to 200 nm in length [105].

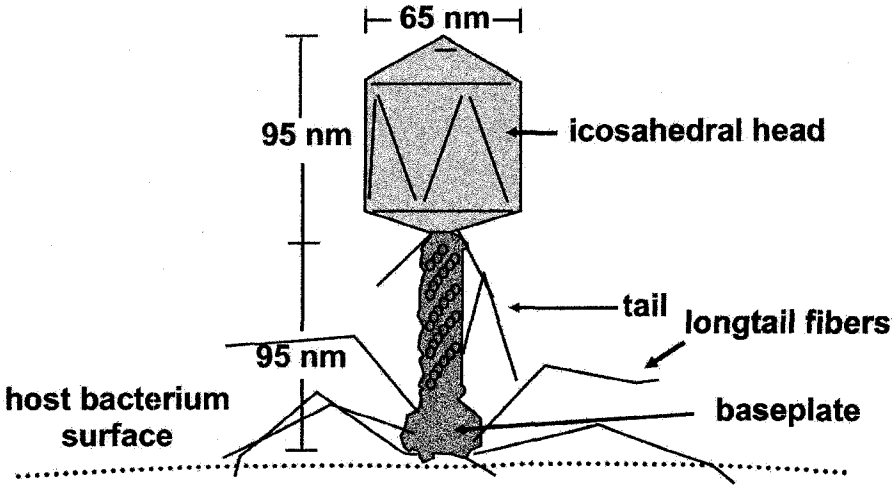

Figure 2.1: T4 bacteriophage structure

The head or capsid present in all bacteriophage serves to protect the nucleic acid that resides within. It can be either icosahedral (20 sided), such as in T4, or filamentous.

The head is composed of copies of one or many different kinds of proteins depending on the complexity of the bacteriophage. Most bacteriophage have a tail used to inject the nucleic acid into the host bacterial cell. The tail is usually composed of a hollow tube core surrounded by a contractile sheat, end plate and tail fibers. The tail fibers determine the specificity to a strain of bacteria. Some bacteriophage have other structures involved in binding such as filaments and enzymes. Proteins and nucleic acid compose most of the bacteriophages structures. The nucleic acid can be either DNA or RNA in several forms (ex.: double stranded, single stranded), but not both. DNA is present in 95% of known phage; RNA accounts for the remaining 5%. The phage genome can have a size of 5 to 650 kilo base pairs (kbp). T4 DNA is about 170 kbp. Simple bacteriophage only have 3 to 5 genes while the most complex ones can have over 100 genes [105, 106].

2.1.2 Infection of Bacterial Cells

Bacteriophage infect host bacterial cells first by adsorbing onto the surface cell wall. Tail fibers or analogous structures connect specifically to bacterial receptors such as lipopolysaccharide (LPS), pili, and lipoprotein. Bacteriophage have evolved to exploit these essential bacterial structures.

As with antibiotics, bacteria can develop immunity to bacteriophage [105, 106]. However, it is considered more complex to do so because resistance to a phage typically results in a mutational loss of a bacteria's specific receptor. This loss generally has a negative effect on the bacteria's survival and does not protect it against phage that bind to different receptors. This effect is exploited in phage therapy where a cocktail of phage that have different receptor specificities are chosen for treatment.

A T4 bacteriophage attached to a bacteria is shown in Figure 2.2. The end plate creates an irreversible attachment and readies the bacteriophage for nucleic acid injection initiated by contraction of the sheath, injecting the hollow tube core through the bacterial envelope. Some phage that lack sheaths use enzymes to pierce the envelope. Nucleic acid is finally injected from the capsid, through the tail, hollow core and into the bacterial cell. The nucleic acid is the only component to enter the cell.

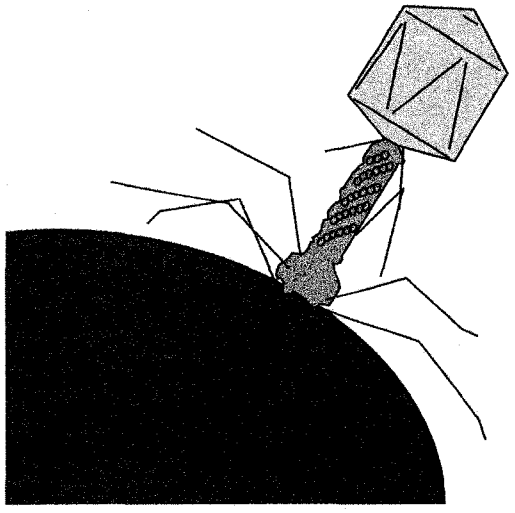

Figure 2.2: T4 bacteriophage adsorbing onto bacteria

2.1.3 Bacteriophage Life Cycle

There are two main types of bacteriophage: the lytic phage and the lysogenic phage [105, 106]. Once lytic phage such as T4 and T7 have adsorbed onto a bacterial cell and injected their DNA, they will begin to produce many copies of viral components. These components are then assembled into complete viruses following which the bacteria is lysed to release the phage and infect other cells.

Temperate or lysogenic bacteriophage such as λ fuse their nucleic acid with that of the host bacteria. The newly combined genetic material, called a prophage stays resident in the host's genome without apparent harm. The genome is passed on to child cells at each subsequent cell division. When the genome senses stress in the environment such as a drastic change in pH, temperature or UV radiation, the bacteria will enter the lytic cycle and produce phage viruses.

Some bacteriophage such as m13 and f1 do not undergo the lytic cycle. These filamentous phage have a circular single-stranded DNA (ssDNA) that is converted to double stranded DNA (dsDNA) in the host cytoplasm. The dsDNA is used to produce phage particles that are secreted out of the bacteria. The bacteria can continue to grow and divide indefinitely with a decrease in the rate of cell growth.

2.1.4 Lytic Bacteriophage

The lytic or virulent phage starts to reproduce upon entering the bacteria. The lytic cycle of a phage is illustrated in Figure 2.3. The phage begins by adsorbing to the bacteria cell wall and injecting its nucleic acid (steps 1 and 2). The phage's nucleic acid overrides the host cell's biosynthetic machinery and begins to make large amounts of viral components (Lytic Cycle path on the right and step 3). In the case of DNA viruses such as T4, the DNA is transcribed to early messenger RNA (mRNA). In the case of retroviral phage such as MS2, R17 and f2, RNA is transcribed by reverse transcriptase into DNA. The DNA is then transcribed to early mRNA [105, 106].

The early mRNA is used by the host's ribosomes to produce phage induced proteins. These proteins are used for phage DNA or RNA synthesis and for turning off the host's DNA, RNA and protein synthesis. Some of these proteins are also used to degrade the host's chromosomes. Late mRNA and late structural phage protein are then synthesized.

When many copies of viral components are synthesized, helper proteins help in the assembly of the bacteriophage (step 4). Base plates are assembled first and the tails are attached to them. The separately constructed capsids self-assemble with the tails. DNA or RNA is packed into the capsid heads. This step takes about 15 minutes.

The phage then produce endolysin, an enzyme which breaks down peptoglycan in the bacteria cell wall. The bacteria is filled with liquid and is broken open to release the bacteriophage to infect new bacteria (step 5). This complete cycle takes about 20 minutes for bacteriophage T4.

The bacteriophage lytic cycle is illustrated in the graph of Figure 2.4. The cycle begins after infection in the eclipse phase. Phage structural and helper proteins and components are made. No infectious phage particles are present inside the bacteria. The bacteria begins to assemble phage structural proteins and nucleic acid in the intracellular accumulation phase. The phage particles increase in number inside the host until they the accumulation of phage lysis protein is sufficient to lyse the host and release the phage in to the medium. The number of phage released can be as high as 1000.

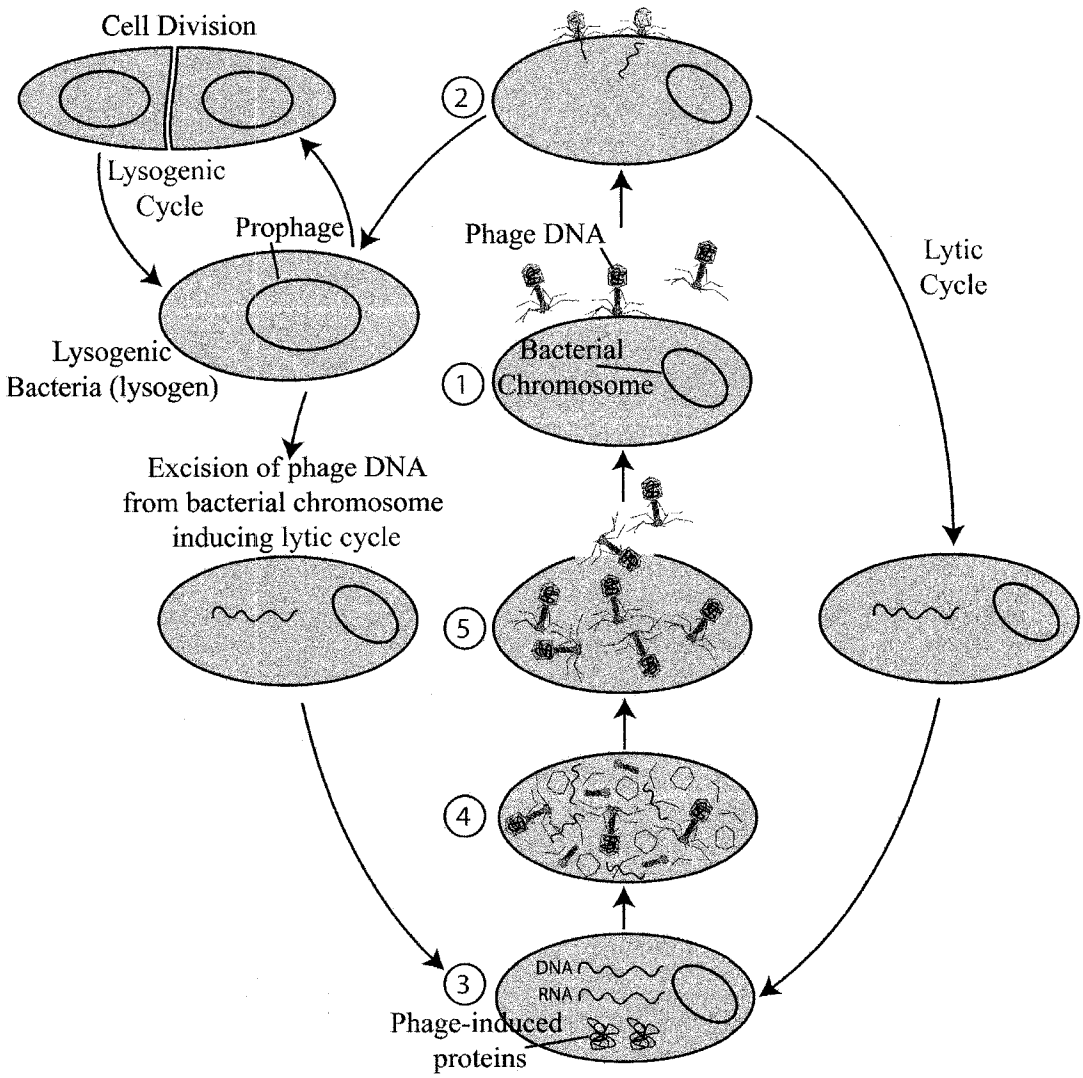

Figure 2.3: Bacteriophage lytic and lysogenic cycles

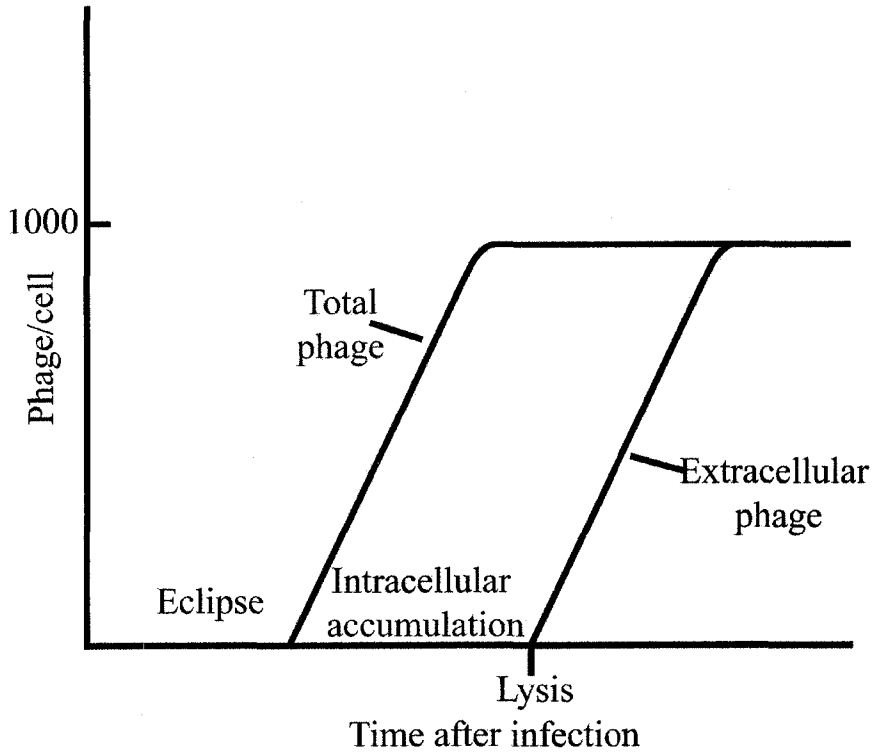

Figure 2.4: Bacteriophage lytic cycle

2.1.5 Lysogenic Bacteriophage

In lysogenic or temperate bacteriophage such as λ, site specific recombination is initiated between specific sites of the circular phage DNA and the host DNA by a bacteriophage enzyme. This results in the integration of the phage DNA into the bacterial DNA as shown in Figure 2.4.

The phage enters the lysogenic cycle. In the prophage state, the bacteriophage's genome is repressed and does not affect the growth of the bacteria. The prophage is not a bacteriophage but has the potential to become one. The prophage is duplicated at each subsequent division as it is passed on to child cells. A repressor protein binds to the operator site on the bacteriophage DNA. This disables bacteriophage reproduction genes and prevents lysis of the host. Each bacteriophage only represses its own genome. If the bacteria is infected by another type of bacteriophage, it will reproduce normally. The DNA of the prophage codes for proteins that wait for signs of stress in the host cell. Stress

caused by starvation, poisons (such as antibiotics), UV light and drastic changes in pH or temperature will cause the production of a protease, rec A protein. This protease disables the repressor protein and leads to bacteriophage gene expression and the beginning of the lytic cycle. The prophage excises itself from the host DNA, degrades the host DNA, produces mRNA and enters the lytic cycle.

2.2 Phage Display

Phage display is extensively used in proteomics to determine protein-protein binding interactions. This is especially useful in drug research to determine antibody-antigen interaction, enzyme action and cell-receptor function.

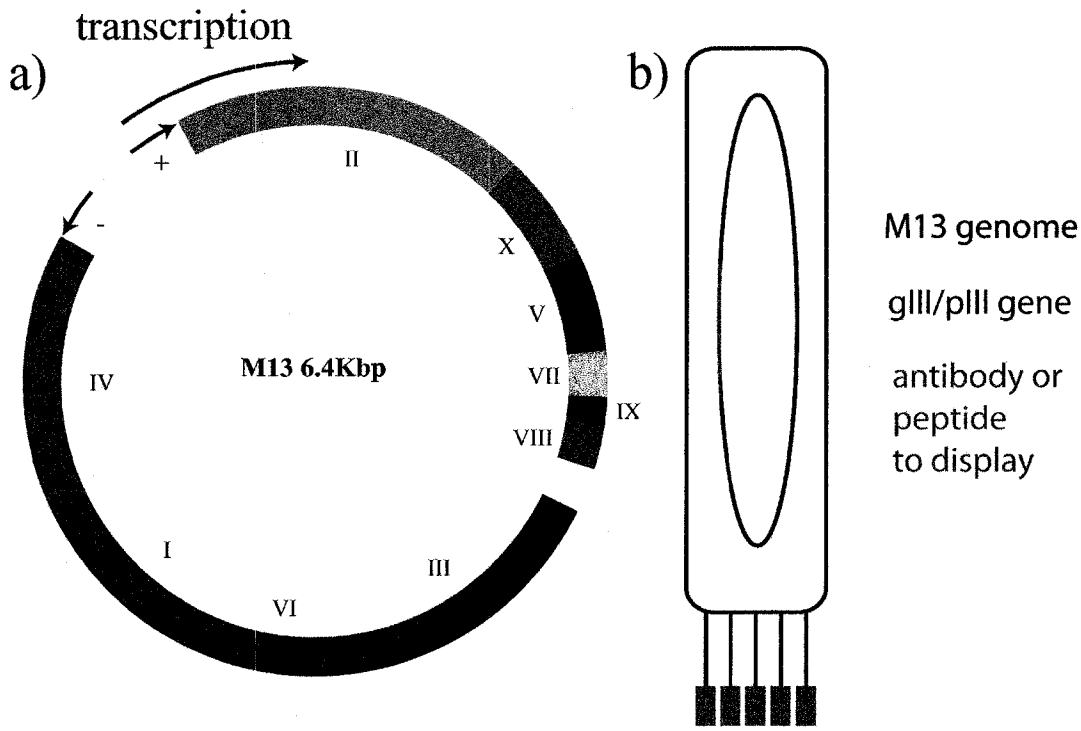

Figure 2.5: Bacteriophage used in phage display a) M13 bacteriophage circular DNA b) Phage display of a peptide or antibody

M13 is a filamentous phage commonly used in phage display [107, 108]. Shown in Figure 2.5a, its circular single stranded DNA is 6.4 kbps long and codes for 10 genes. Gene VII encodes for major structural proteins and gene III encodes for minor coat proteins. In

Figure 2.5b, a DNA sequence is cloned in frame with gene III. This DNA sequence encodes for a short peptide chain that is displayed on the surface of the bacteriophage.

In phage display shown in Figure 2.6, a protein is coated onto a substrate. Random proteins are displayed onto the coats of bacteriophage. A phage library is a collection of these bacteriophage containing a vast amount of variations of proteins. Libraries can contain millions of different phage with different proteins displayed on each phage.

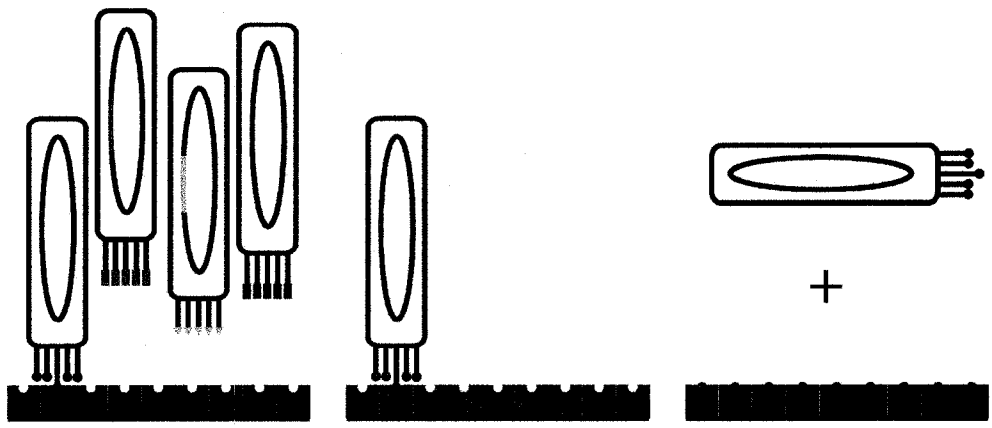

1. The substrate is coated with target protein and exposed to a phage library

2. Unbound phages are washed away

3. Specifically bound phages are eluted by a change in pH or an excess of a known ligand to the target

Figure 2.6: Phage Display

The phage library is transfered onto the substrate. Some bacteriophage coat proteins will interact with the substrate proteins. The substrate is washed with a buffer solution. The bacteriophage with strong protein interactions will remain. Non-interacting bacteriophage will be washed away. Specifically bound phage are eluted by a change in pH or by washing the substrate with an excess of a a known ligand protein to the target.

Eluted bacteriophage are amplified and cloned. The bacteriophage DNA is then extracted and sequenced to determine what proteins interacted with the substrate protein. Various kinds of phage can be used for phage display. The maximum insertion length of the display protein is determined by the size of the bacteriophage genome. Large phage

allow DNA cloning of large proteins. The smallest phage commonly used in phage display is M13 or f (6.4 kbp) followed by T7 (40 kbp), λ (49 kbp) and T4 (169 kbp), which allows for very large proteins to be displayed.

2.3 Bacteriophage for Biosensing

While antibodies are commonly used as specific recognition probes, they are expensive to produce and are very sensitive to degradation from temperature, pH and cross reactivity. Bacteriophage show great promise in the development of biosensors where they can be used to specifically detect proteins and bacteria. Bacteriophage are easy and cheap to produce in large numbers and show great specificity to target bacterial species. This makes them ideal recognition probes for biosensors.

Phages have the added advantage of only binding to live bacteria. This contributes to reduce the number of false positives that would arise from using antibodies or PCR techniques that can detect and bind both dead and living bacterial cells. There have been increased interest in developing phage based biosensors, as shown by several examples in the literature.

Egar *et al.* have detected bacteria using streptavidin coated quantum dots bound to biotin labeled phage [109]. An epitope biotinylation site is displayed onto a phage. A solution of these phage is injected into a bacterial solution. The lytic cycle produces many phage inside of each bacteria and these phage are biotinylated by the biotin ligase protein. Biotinylated phage bind to streptavidin coated quantum dots that are detected by fluorescent microscopy and flow cytometry.

Dobozi-King *et al.* have developed a method to detect bacteria by sensing a phage triggered ion cascade using a micro-fabricated quantum well [110, 111] When a phage infects a bacteria, a pore is created in the bacterial cell wall. An estimated 100 million ions flow out of the cell. This process varies the voltage between the plates of a micro-fabricated capacitor. This sensor has the ability to detect live bacteria with a detection time of 10 minutes.

Bacteriophage pathogen detecting biosensors are evolving in the direction of using phage adsorbed to a surface as recognition probes. Nanduri *et al.* physically adsorbed landscape

phage onto the surface of a quartz crystal microbalance (QCM) to detect beta-galactosidase from *E. coli* [112]. Balasubramanian *et al.* have developed an SPR biosensor capable of detecting *Staphylococcus aureus* at a concentration of 10^4 cfu/mL using lytic phage immobilized by physical adsorption onto the gold surface of the sensor [113].

Promising research has been undertaken to develop sensors using bacteriophage as specific biodetection probes. The majority of these sensors use fluorescent labeling techniques or physical adsorption of phage onto surfaces to detect bacteria. The ability to chemically immobilize phage onto surfaces can create surfaces with a greater density than physical adsorption alone. In addition, attachment of phage with tails facing upwards would ensure that more receptors are positioned appropriaptly to capture bacteria. The chemical binding of phage to biosensors can create sensors that are much more sensitive than biosensors using physically adsorbed phage.

3

Building Blocks For Bacteriophage Immobilization

Bacteriophage are highly desirable recognition probes for biosensensing. Bacteriophage have been physisorbed onto biosensor surfaces [112, 113]. These sensors exhibited low binding densities of bacteriophage and did not prevent the non-specific binding of bacteria. By tuning the biosensor surface to chemically immobilize bacteriophage, the density and orientation can be improved and non-specific binding can be minimized.

Chemical functionalization procedures to be used in immobilizing bacteriophage will be introduced. Self-assembled-monolayers (SAMs) are commonly used to chemically modify the chemical properties of bioMEMS interfaces. SAMs can be used to modify hydrophobicity, functional groups for specific binding of proteins and to minimize non-specific binding. Finally, the biotin and streptavidin complex is the strongest known non-covalent binding system for biological cells and molecules.

3.1 Self-Assembled Monolayers

Nanotechnology requires surfaces that are engineered at the molecular level. Biological systems specifically demand surfaces that are compatible with cells and proteins. Self-

assembled monolayers are molecular thick films or organic compounds on surfaces. SAMs bind to surfaces by forming strong covalent bonds between the tail group and the substrate. The head group of the SAM is left free for binding to other different compounds. SAMs have become an indispensable tool for modeling and designing biological surfaces for biosensors [114–116], tissue engineering [117] and fundamental biological studies [118].

SAMs provide an easy way to immobilize molecules on a multitude of different substrates. Ordered, pinhole free and stable monolayers are easily formed. Monolayers provide membrane-like environments that are suitable for biomolecule immobilization. SAMs can be terminated by various head groups and tail groups to change the binding properties of the monolayer allowing the design of hydrophobic or hydrophylic surfaces. Only a minimum of biomolecules is needed (a monolayer) for further functionalization onto the SAM terminated substrates. The surface of SAMs are relatively stable, allowing for several reliable measurements of protein absorption, antibody-antigen interaction and DNA hybridization [119].

However, SAMs also have some limitations. Immobilized enzymes can be sensitive to pH, strong ion solutions and temperature. Some thiol SAMs can be chemically oxidized, desorbed electrically or thermally. This must be considered carefully in the design of biosensors but can also be used advantageously to regenerate surfaces [119].

3.1.1 Self-Assembled Monolayer Formation

Disulfides, sulfides, and thiols chemisorb very strongly to coinage metals such as gold, silver, platinum or copper. Sulphur containing compounds have a strong affinity for noble metals. A gold substrate in the presence of an alkenethiol solution or vapour will form a SAM. Thiolate is formed by oxidative addition of the S-H bond on the gold substrate, followed by reductive elimination of the hydrogen [120]

$$R - S - H + Au(0)_n \Rightarrow R - S^- Au^+ Au(0)_n + \frac{1}{2}H_2 \tag{3.1}$$

Gold is easy to handle because it doesnt have a stable oxide. Thiolated gold substrates are biocompatible and are stable in air, water or ethanol for several months. However, they desorb at 70°C, when irradiated with UV light and in the presence of oxygen or

ozone [121]. Thiols on gold are ubiquitously used in biosensors. Silver substrates provide an almost equally attractive structure for SAMs but the cytotoxity of Ag^+ ions makes them unusable in biological applications [120].

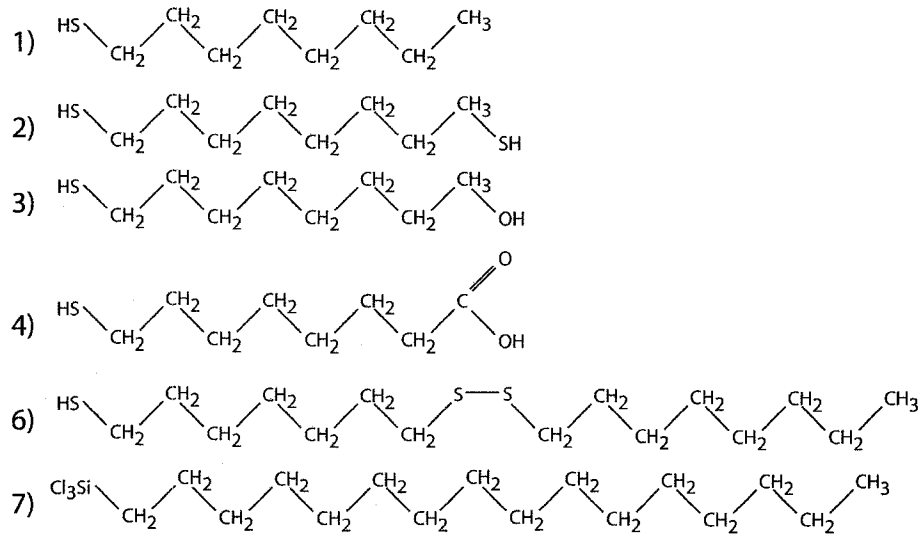

Figure 3.1: Common self-assembled monolayers

Common SAMs are shown in figure 3.1. SAMs 1) to 4) are thiols with different functional groups: methyl, sulfo, hydroxyl and carboxyl respectively. SAM 6) is a disulfide that spontaneously cleaves at the sulfur bond to bind to gold similarly to thiols. SAM 7) is a silane with a methyl functional group.

Alkylsiloxanes are obtained by reacting an alkyltrichlorosilane solution with a hydroxylated surface (SiO_2 or silica glass). The silane group hydrolizes to form silanol, then slowly condenses to oligomers and finally hydrogen bonds to the surface hydroxyl groups to form covalent bonds. These SAMs show significantly stronger stability than alkanethiolates on gold and do not require deposition of a metal layer. This can be advantageous in cantilevers as deposited gold thin films can reduce the Q factor by an order of magnitude [122]. However, silanes do not form as dense and well ordered monolayers as thiols [120].

Dense monolayers assemble quickly but take several days to form well ordered monolayers. Monolayers show biphasic assembling kinetics: diffusion-controlled adsorption is followed by a slow recrystillisation phase. During the alkanethiol monolayer

adsorption phase a densely packed monolayer is formed in less than one hour. The monolayer is stabilized by strong van der Waals interactions between the alkyl chains. Following this the monolayers slowly recrystallizes. After six days of immersion, multilayer formation is observed [121].

3.1.2 Applications of Self-Assembled Monolayers

Proteins tend to adsorb more to substrates with greater hydrophobicity. Protein and cell adsorption is not always desired, as there are biological entities that are not required to bind. Non-specific adsorption can create noise and false results. Thus there is a need for SAMs that resist the adsorption and adhesion of biological entities. Inert SAMs include oligo(ethylene glycol) or poly(ethylene glycol) and mannitol-terminated SAMs. These inert monolayers are highly resistant to small proteins but show difficulty in preventing the adsorption of larger proteins and cells [123].

Mixed monolayers of reagents of different chain length show ideal mixing. The resulting monolayer depends on the relative rate of adsorption of the components. The resulting SAMs is relatively homogenous and does not phase segregate into islands. Mixed monolayers can be especially useful to enhance protein binding [124]. Streptavidin binding on a pure monolayer was found to be hindered. Preparing the SAM with a mixture of thiols of the same length did not improve binding much. However, a mixed monolayer of different lengths was found to add space between binding sites and prevent steric hindrance, increasing the binding efficiency of streptavidin.

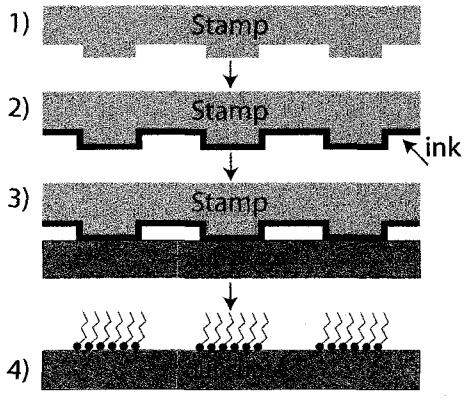

Figure 3.2: Microcontact printing

Several techniques have been developed to pattern SAMs onto subtrates for biological application. Microcontact printing uses a poly(dimethylsiloxane) PDMS stamp inked with an alkanethiol to transfer patterned SAMs to a gold substrate as shown in figure 3.2 [125]. In dip pen lithography, an alkanethiol coated AFM tip can be used. A water meniscus solubilizes some of the alkanethiol and forms a monolayer on the substrate as shown in figure 3.3 [126]. Patterning using lithography and microfluidics channels have also been achieved [127–129].

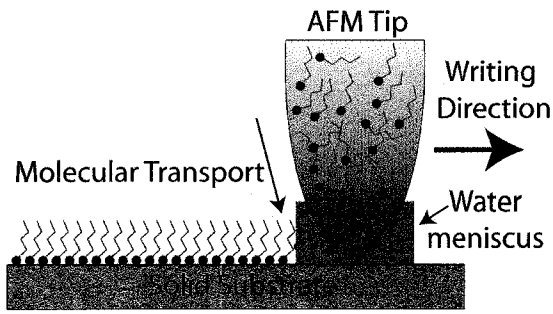

Figure 3.3: Dip pen nanolithography

Antigens have been detected using SAM covered QCM sensors [130, 131]. Antibodies were covalently bound to SAMs. Bovine serum albumin (BSA) is used to block non-specific binding. Functionalized QCM sensors are capable of the high-throughput detection of different antigen-antibody binding events.

3.2 Biotin-Avidin Complex

To effectively immobilize biological molecules such as bacteriophage to surfaces it is important to use an efficient binding mechanism. The biotin-avidin system is one of the most well studied and used biological system. Avidin has four biotin binding sites that can be used to crosslink between different biotinylated biological entities. In addition, avidin can be coupled to different ligands such as enzymes, fluorochromes and tethers making the bioton-avidin system useful in a variety of biological binding applications.

Biotin, also known as vitamin H, Bw or coenzyme R, is found naturally in all living cells. The pancreas, liver and kidney contain the largest quantity of biotin in the human body [132]. Biotin is a carbon dioxide (CO_2) carrier used during glycogen formation,

amino acid metabolism and fat synthesis. Biotin is present in many vegetables and meats and is synthesized by intestinal tract bacteria such as *E. coli* [133, 134].

Avidin is found in bird, amphibian and reptile tissue and in eggs. Avidin is a 67 kDa glycoprotein that consists of four identical 128 amino acid subunits. Approximately 10% of the structure of avidin is composed of carbohydrates [134]. Because avidin can cause high non-specific binding, streptavidin is often used instead. Streptavidin isolated from *S. avidinii* bacteria consists four subunits of 159 amino acids and contains no carbohydrates. Neutravidin is another commonly used form of avidin that is fabricated by deglycosylating native avidin [135]. The Neutravidin protein contains no carbohydrates and has a modified surface charge that leads to a more neutral isoelectric point.

The binding of biotin and avidin form a robust non-covalent bond that resembles antigen-antibody binding. The bond is extremely stable resisting organic solvents, denaturing agents and extreme temperatures and pH [135]. Strong hydrogen bonds, van der Waals forces and conformational changes make the interaction between biotin and avidin nearly irreversible. The binding constant K_a of biotin-avidin is considered extremely high at 10^{15} M^{-1}.

Table 3.1: Properties of different avidin forms

	Avidin	Streptavidin	NeutrAvidin
Molecular Weight (kDa)	67	53 - 60	60
Isoelectric Point (pH)	10 - 10.5	5 - 7.5	6.3
Biotin Binding Constant K_a (M^{-1})	10^{15}	10^{13} - 10^{15}	10^{15}
Non-specific Binding	High	Low	Lowest

Shown in table 3.1 are the properties of the different forms of avidin. Streptavidin and neutravidin have lower molecular weight than avidin because of the removal of the carbohydrate. The binding efficiencies are nearly identical with some variation for streptavidin [135]. Streptavidin and neutravidin have lower isoelectric points which contributes to reduce non-specific binding.

There are a wide variety of biotinylated compounds available making the biotin-avidin system highly amenable to biological recognition on surfaces. Commonly, biotin is immobilized onto the surface of the transducer. Biotin can be immobilized by chemisorbtion or crosslinking. Chemisorbtion involves using a biotinylated thiol or

disuphide SAM. Crosslinking is also possible. A SAM with a suitable terminal group is bound to a gold surface followed by the chemical coupling of a biotin derivative [136, 137]

Patterned SAMs have been used in to detect protein-DNA interactions using SPR [138]. A biotin containing mixed self-assembled monolayer was used to bind streptaviding protein and biotinylated dsDNA. The mixed SAM was produced from biotin and olig(ethylene glycol) terminated thiols. An ideal streptavidin binding layer with $5x10^{12}$ binding sites/cm^2 was produced allowing the dense immobilization of biotinylated molecules.

Different biotin terminated thiols were immobilized on gold and characterized using SPR [139]. Increasing the length of the alkyl chain separating the head and tail groups of the thiols was found to reduce the non-specific interaction between the streptavidin and the surface and increase the specific binding of streptavidin to the biotin groups.

There are several examples of MEMS biosensors that employ SAMs that were covered in chapter 1. One such example is an *E. coli* amperometric sensor [116]. A detector array was fabricated with multiple electrodes. Biotin terminated SAM were immobilized onto a gold electrode onto which streptavidin was bound to capture *E. coli* rRNA. Using a biotinylated thiol yielded the best results over streptavidin physisorption and biotin disulfide.

3.2.1 Conclusions

Self-assembled monolayers are a powerful tool to modify sensor surfaces. They can be used to modify hydrophobicity and hydrophylicity. SAMs with chosen functional groups can be used to bind desired biological entities or they can be used to minimized non-specific binding of cells and proteins.

The biotin-avidin system is an extremely stable and versatile way to immobilize biological entities to surfaces. Many biological entities such as cells, proteins and nucleic acids can be biotinylated and bound efficiently to immobilized surfaces.

In the following chapter, self-assembled monolayers and the biotin-avidin system will leveraged to bind biotinylated bacteriophages to substrates for bacterial detection in bioMEMS.

4

Bacteriophage Attachment Chemistry

The chemical attachment of phage onto sensor surfaces can significantly improve the stability and performance of phage based biosensor platforms. This can also enable the employment of phage in applications where patterning of the probing element is required.

Chemical biotinylation of phage has been shown to significantly increase the efficiency of phage-based biosorbents when compared to simple physical adsorption. Sun *et al.* have used biotinylated phage coated onto streptavidin labeled magnetic beads to capture bioluminescent *S. enterditidis* bacteria [140]. The procedure is shown in Figure 4.1. Their results have shown that the number of cells captured using the phage coated beads is five times that of beads coated with non-biotinylated beads.

Similarly to the bead approach, bacteriophage bound from the head capsid protein onto a microsensor surface would allow the tail fibers and baseplate to face the medium, enabling a more efficient capture of bacteria.

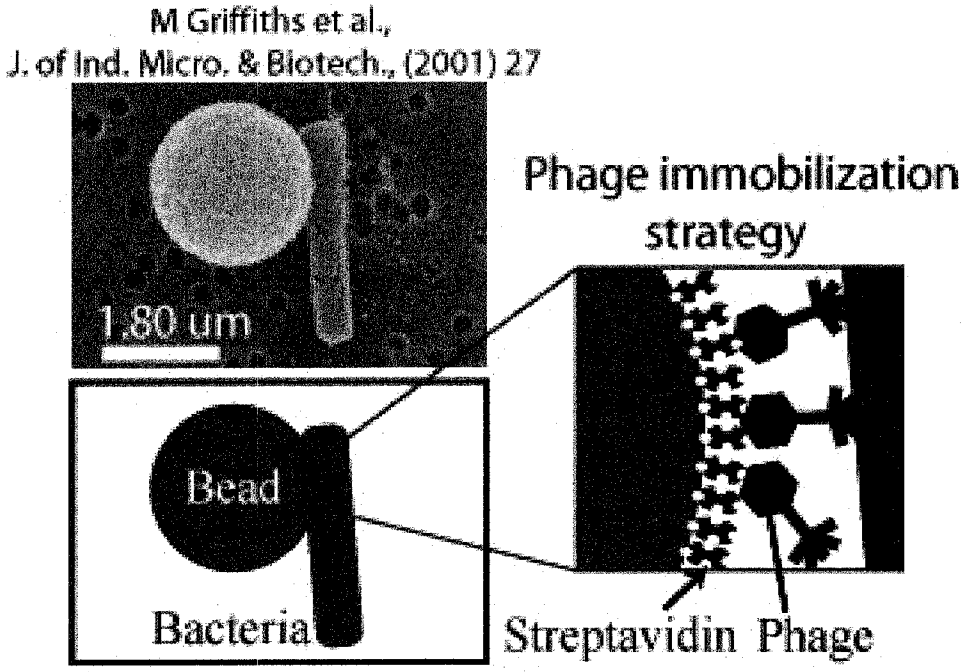

Figure 4.1: Bacterial capture using bacteriophage coated magnetic beads [140]

Described here is a chemical attachment scheme that leverages T4 bacteriophage that are genetically engineered to express biotin on a capsid protein [141]. These bacteriophage express biotin directly on a capsid protein and do not require biotin to be artificially bound to them. As opposed to phage biotinylated by chemical procedures, the biotin is in this case exclusively present on the phage capsid, and not on their tail.

An alternative approach has been presented in recent literature [109]. A T7 phage is genetically engineered to display a small biotinylation peptide on the major capsid protein. Bacteriophage that infect the host bacteria are biotinylated by the biotin-ligase protein (BLP) that is present in all living cells. Biotin is attached by the BLP to a specific lysine residue in the tagged peptide.

The biotin-avidin complex has been used and previously reported in bacterial sensing applications [142, 143]. Reported here is the streptavidin-mediated attachment of genetically-modified biotinylated phage onto gold electrodes as shown in Figure 4.2.

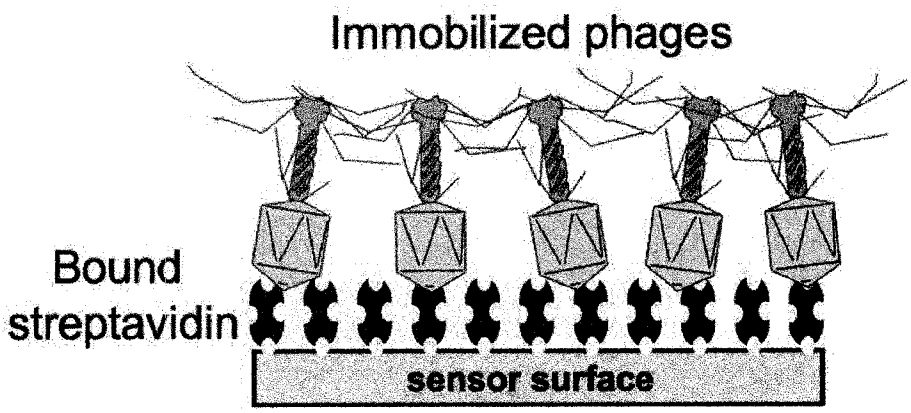

Figure 4.2: Streptavidin-mediated attachment of genetically biotinylated T4 bacteriophage onto gold electrodes

This attachment chemistry is then employed to capture bacteria on an impedance biosensing device's gold electrode as shown in Figure 4.3. The well characterized T4 phage is chosen as a model system. T4 bacteriophage is known to be highly specific to *E. coli* as it binds highly selectively to *E. coli* B-type lipopolysaccharide or OmpC protein [144–146]. T4 only infects *E. coli* and the closely related *Shigella* species and thus is considered to have a very narrow host range [147, 148]. We observe that such streptavidin-mediated attachment of these biotinylated phage significantly delays the growth of the host bacterium in comparison with electrodes functionalized using wild type phage.

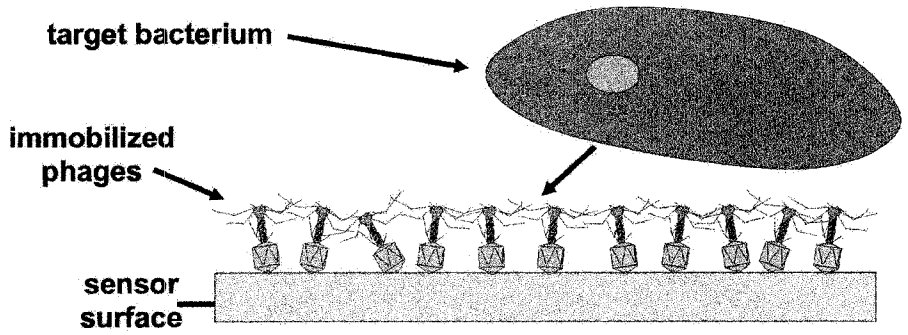

Figure 4.3: Bacterial capture on impedance sensor gold electrode

Such antibody-free chemical attachment of phage onto sensor surfaces could therefore be used in numerous other sensing transduction techniques, and enable the design of

highly sensitive and highly specific platforms for the detection and identification of host pathogenic organisms.

4.1 Materials and Methods

1-Hexadecanethiol, 11-Mercapto-1-undecanol, 11-Mercapto-undecanoic acid, Cysteamine Hydrochloride and Bovine Serum Albumin (BSA) were purchased from Sigma-Aldrich (St-Louis, Mo, U.S.A.). Sulfosuccinimidyl 2-(biotinamido)-ethyl-1,3-dithiopropionate (Sulfo-NHS-SS-Biotin), tetramethyl rhodamine isothiocyanate (TRITC)-conjugated streptavidin and BupH Phosphate Buffered Saline Packs were purchased from Pierce (Rockford, Il, U.S.A.). *E. coli* was labeled using the SYTO BC bacteria stain from a bacteria counting kit purchased from Invitrogen (Carlsbad, Ca, U.S.A.). Electric cell-substrate impedance sensing (ECIS) 8W1E chips were purchased from Applied Biophysics (Troy, NY, U.S.A.). *E. coli* ATCC 11303 and wild type T4 bacteriophage were obtained from Biophage Pharma Inc. (Montreal, Canada). T4 bacteriophage with biotinylated capsid heads were provided by Dr M. Griffiths (University of Guelph, Canada).

Luria Bertani (LB) media was purchased from Quelabs (Montreal, Canada) and prepared by dissolving 25 g of LB powder into 1 L of distilled water. LB-agar medium was prepared by adding 6 g of granulated agar in 400 mL of LB media. TSB media was prepared with 211825 Bacto TrypticSoy Broth (Fisher Scientific) by following the instructions of the manufacturer. For suspending bacteria, 5% TSB solution was prepared by adding 2.5 mL of the TSB media to 47.5 mL of 0.15 M NaCl. Lambda or SM buffer was prepared using Sigma reagents by diluting 5.8 g NaCl, 2.0 g $MgSO_4$-$7H_2O$, 50 mL 1M Tris-HCl at pH 7.5, 1 mL 10% (w/v) gelatin in 1 L of distilled water. The LB medium and SM buffer were autoclaved. Phosphate buffered saline solution (PBS) was prepared by mixing one BupH phosphate buffered saline pack to 500 mL of MilliQ water yielding a solution of 0.1 M phosphate, 0.15 M NaCl, pH 6.9 - 7.2. The lambda buffer employed for phage suspension was prepared by mixing 5.8 g NaCl, 2 g $MgSO_4.7H_2O$, 50 mL 1 M Tris, 1 mL of 10% gelatin, and adding 1000 mL of distilled water.

4.1.1 Culture and Labeling of Bacteria

Bacterial stock culture was prepared by suspending an isolated colony from a bacterial plate into 4 mL LB media. The inoculated LB was then incubated overnight at 37°C in an incubator-shaker. Log-phase bacterial culture are then freshly prepared each day from the stock culture: 200 μL of stock culture was inoculated into 4 mL LB media and incubated for 2 hours at 37°C in an incubator-shaker. Enumeration of bacteria was performed by the plate count technique and expressed in colony forming units (cfu/ml). The procedure typically yielded a bacterial density of 10^8 cfu/ml and was used for bacterial adsorption experiments and phage amplification. For the bacterial adsorption experiments, 1 mL of the bacterial culture was collected by centrifugation at 5000 rpm for 5 min. Bacteria were then resuspended in 5% TSB solution. Finally 1 μL of SYTO BC bacterial stain B7277 (Component A, Invitrogen) was added to the solution and incubated for 5 min. at room temperature.

4.1.2 Bacteriophage Amplification

Amplification of the phage was performed by using established methods. 10^5 plaque forming units (pfu) of phage preparation was mixed with 10^6 cfu of fresh log-phase E. coli ATCC 11303 bacterial culture. After 15 min of incubation at room temperature, LB medium was added to the mixture followed by a 6 h incubation in a shaking incubator at 37°C. The solution was then centrifuged at 4000 g to pellet the bacteria. The supernatant was filtered using a 0.22 μm filter to remove any remaining bacteria. The filtered supernatant solution was then concentrated by ultracentrifugation at 60 000RPM for 1 h, and the phage pellet was resuspended in 1 mL SM buffer. Since the pellet was not visible, the tube was kept at an inclined position such that the buffer was covering the area where the pellet was expected to exist. The tubes are kept in this position overnight at a temperature of 5°C. Enumeration of phage was performed by the soft agar overlay technique and expressed in pfu/ml [149]. Phage concentrations reaching 10^{11} pfu/mL were routinely obtained.

4.2 Streptavidin Immobilization Chemistry Development

Our phage immobilization procedure leverages the presence of biotin on the phage capsid, and the natural affinity of the biotin/streptavidin system. A series of binding procedures have therefore been investigated to optimize the attachment of streptavidin onto gold while minimizing the non-specific binding of the host *E. coli.* Substrates were fabricated with a 3" silicon (111) wafer by first sputtering 5 nm of a chrome adhesion layer followed by 50 nm of gold. The coated wafer was then cleaved into 5 mm x 20 mm rectangles using a diamond tip pen. Six of these gold surfaces (A to F) were then immersed in 1 mM self-assembled monolayer solutions for 24 hours. More specifically, samples A and B were immersed in 1-Hexadecanethiol diluted in ethanol. Additionally, sample B was also immersed in Bovine Serum Albumin (BSA) dissolved in phosphate buffer pH 7.2 with a concentration of 1 mg/mL. BSA is used to block the surface to potentially reduce non-specific adsorption of the bacteria to the 1-Hexadecanethiol. Sample C was immersed in 11-Mercapto-1-undecanol diluted in ethanol. Sample D was immersed in 11-Mercapto-undecanoic acid diluted in ethanol. Sample E was immersed in Cysteamine Hydrochloride diluted in ethanol. Sample F was immersed in Sulfo-NHS-SS-Biotin diluted in MilliQ water. Sample G consists of a control surface of bare Au that was not functionalized by any monolayer. The samples were then rinsed in MilliQ water. A diagram of these seven samples is shown in Figure 4.4a.

The seven samples were then treated with a 25 μg/mL TRITC-conjugated streptavidin solution in milliQ water for 15 min. TRITC has absorbance maxima between λ = 515-520 nm and λ = 550-555 nm and an emission maximum at λ = 570 nm. Fluorescence microscopy has been performed using an approach similar to the procedure reported by Huang *et al.* [150]. For this purpose, the substrates were first placed within a durable silicone gasket. An imaging chamber was formed by pressing a square patterned silicone gasket against a microscope slide. The imaging chamber was sealed with a coverslip before taking the fluorescent images and filled with 300 μL of 5% TSB prevent sample dehydration during fluorescence microscopy observation. An Olympus IX81 (Tokyo, Japan) equipped with a TRITC filter and a Roper Scientific CoolSnaps HQ CCD camera (Duluth, Georgia, U.S.A) was then used for recording the fluorescence images.

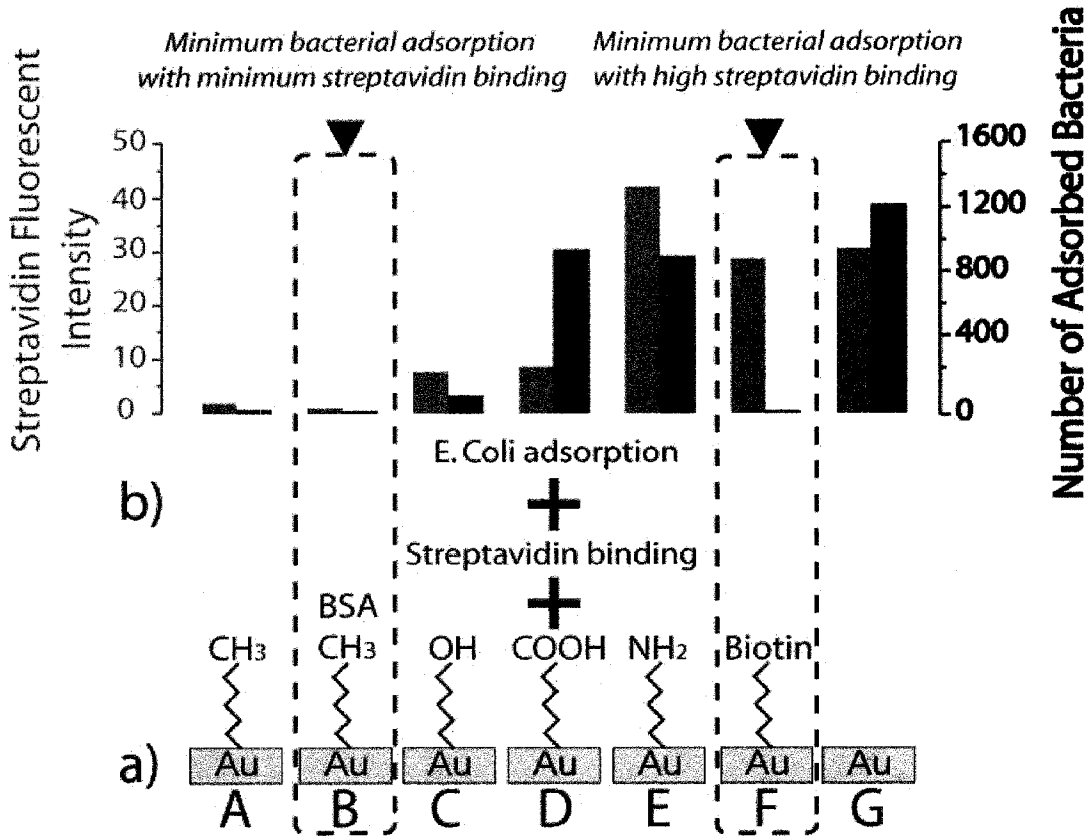

Figure 4.4: Streptavidin functionalization a) Seven gold substrates (A to G) were terminated with various functional groups b) the samples were treated with TRITC-conjugated streptavidin, and SYTO BC *E. coli* and then measured for fluorescence. Sample F, a biotin-terminated alkyl chain, shows high streptavidin binding with minimal non-specific bacterial adsorption, proving to be optimal for the immobilization of biotinylated bacteriophage

Fluorescence intensity has been acquired randomly on 10 different locations for each sample, and averaged. The substrates were then treated with SYTO BC labeled *E. coli* for 15 min at a concentration of 10^8 colony forming units (cfu)/mL, and observed again with the fluorescence microscope. SYTO BC stain has an excitation maximum at $\lambda = 480$ nm and an emission maximum at $\lambda = 500$ nm.

Figure 4.4b shows the fluorescent microscopy data of the 7 gold samples following exposure to TRITC-streptavidin and SYTO BC *E. coli* solutions, respectively. The bacterial count is performed over a 665 μm by 890 μm area. Relative intensity of streptavidin fluorescence as well as bacterial count for each of the 7 samples, are plotted. Streptavidin

and *E. coli* adsorb readily to bare gold (sample G), demonstrating the need of surface chemistry to prevent non-specific adsorption. Hexadecanethiol treated with BSA (sample B) resulted in minimal *E. coli* adsorption coupled with minimal streptavidin adsorption, making it a good candidate for a blocking surface. Bare Hexadecanethiol (Sample A) was also shown to be a good inert surface but to a lesser extent than sample B. The carboxyl- and amine- terminated SAMs (samples D and E) are negative and positively charged surfaces respectively. The isoelectric point can be used to determine the binding affinity of proteins to these surfaces. Streptavidin with an isoelectric point of 5 to 7.5 and Neutravidin with an isoelectric point of 6.5 will both binds more readily to the negatively charged amine substrate E. Avidin has an isoelectric point of 10 to 10.5 and thus will bind more readily to the positively charged carboxyl terminated substrate D. However, these two surfaces also featured significant *E. coli* binding activities that would impede on the specificity of the eventual sensing platform. The hydroxyl terminated SAM (sample C) had much lower adsorption of both streptavidin and *E. coli* Finally, the biotin-terminated SAM (sample F) showed high streptavidin binding with minimal non-specific *E. coli* adsorption, proving to be the optimal candidate for the immobilization of biotinylated phage and thus was used in the following phage termination experiments

4.3 SEM of Phage Terminated Surface

Similarly to the protocol used above, gold substrates were treated with 1 mM Sulfo-NHS-SS-Biotin in MilliQ water for 24 h, and then immersed in 25 μg/mL TRITC-conjugated streptavidin in milliQ water for 15 min. Substrates were then immersed overnight into 10^9 pfu/mL solutions of either wild type or biotinylated phage. The surfaces were then observed with a Hitachi S-4800 (Tokyo, Japan) scanning electron microscope (SEM).

Figure 4.5 shows typical scanning electron micrograph images of the surface following this attachment. Phages are seen as dark objects with a globular head of 100 nm in diameter and a tail of 100 nm in length. Surface densities of 5-10 phage/μm^2 were observed (Figure 4.5a) when biotinylated bacteriophage were immobilized on the streptavidin-coated surface. When considering the size of the host *E. coli* bacteria (0.5 x 2 μm), the density of immobilized biotinylated phage will be sufficient to enable the interaction of phage with

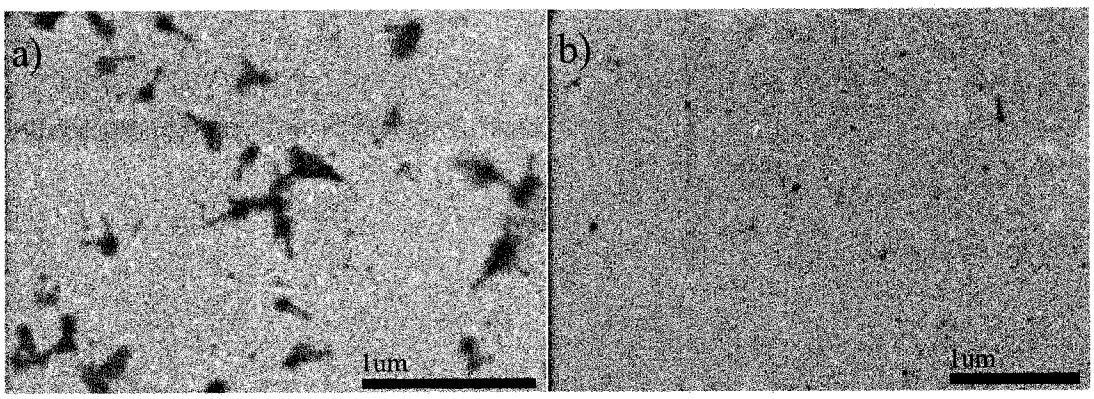

Figure 4.5: SEM of functionalized gold surfaces following attachment of a) biotinylated T4 bacteriophage, and b) wild type T4 bacteriophage.

the bacteria at the interface of the gold layer. In addition, this capture efficiency dropped to less than 1 phage/μm^2 when the wild type phage were used instead of the biotinylated ones (Figure 4.5b). This indicates that the usage of biotin-streptavidin interaction chemistry significantly improves the attachment of the viruses onto the gold surfaces.

4.4 Electrical Cell Impedance Sensor (ECIS)

The attachment procedure described above was used to investigate the effect of a bacteriophage terminated surface on the growth of the bacteria. This assessment was conducted in an Electrical Cell Impedance Sensor (ECIS) device. This device monitors the growth of bacteria by tracking the induced increase in impedance between two electrodes shown in Figure 4.6a. This increase of impedance is mainly related to a constriction of the ionic current allowed to flow as the bacteria increasingly cover the test electrode. Additional impedance signal is however also expected from the growth of the bacteria in the supernatant culture medium itself (Figure 4.6b).

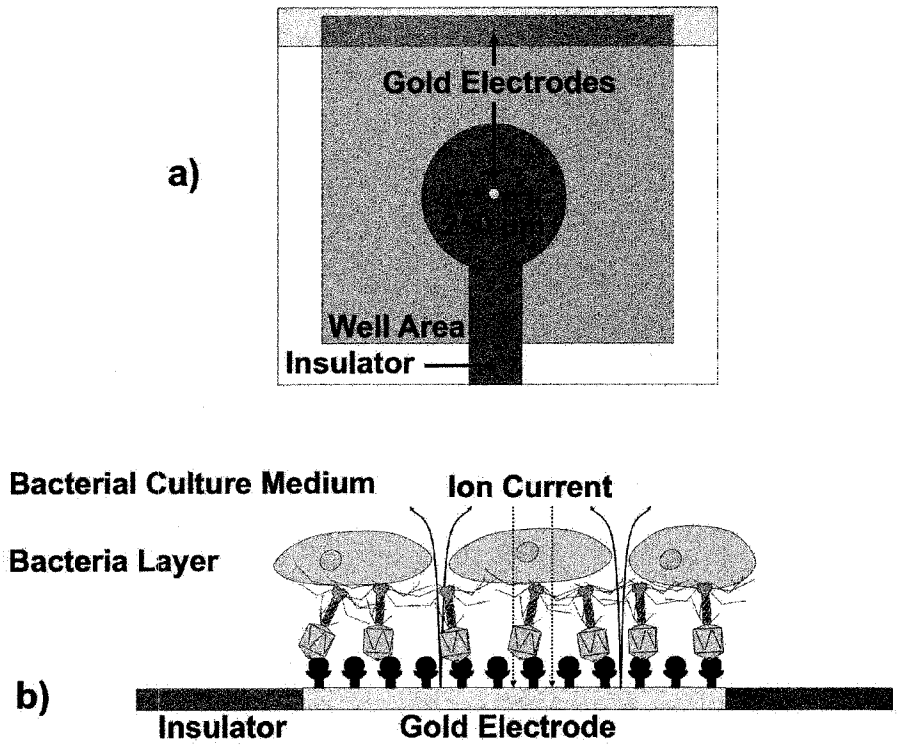

Figure 4.6: Schematic view of an ECIS chip a) well area with reference electrode and 250 μm test electrode b) side view of 250 μm electrode. The test electrode is terminated with Sulfo-NHS-SS-Biotin, streptavidin and biotinylated T4 phage. *E. coli* binds to the surface and grows in an increasingly thick layer that restricts the flow of ion current and increases the measured impedance. Additional impedance signal is also expected from the supernatant culture medium itself.

ECIS was chosen as a well understood technique to study bacterial cell growth in the presence of different culture conditions. Conditions known to produce reliably measurable results were chose to demonstrate the effects of the bacteriophage functionalization chemistry and not to demonstrate the viability of this system as a biosensor.

As was employed for sample F described above, modified ECIS wells were first treated with 1 mM Sulfo-NHS-SS-Biotin in MilliQ for 24 hours and TRITC-conjugated streptavidin for 30 min. Some of the devices were then treated for 30 min with 10^8 pfu/mL of genetically-modified biotinylated phage (T4B), and some with wild type phage (T4W). The devices were then washed twice in PBS and twice in LB. The T4W control experiment was performed to demonstrate the improved performance of the biotinylated phage over

the wild type phage in the presence of the streptavidin-terminated surface. The wells were then filled with the *E. coli* suspension (10^4 cfu/mL), incubated at 37C, and the growth of the bacteria monitored by measuring impedance for 24 h.

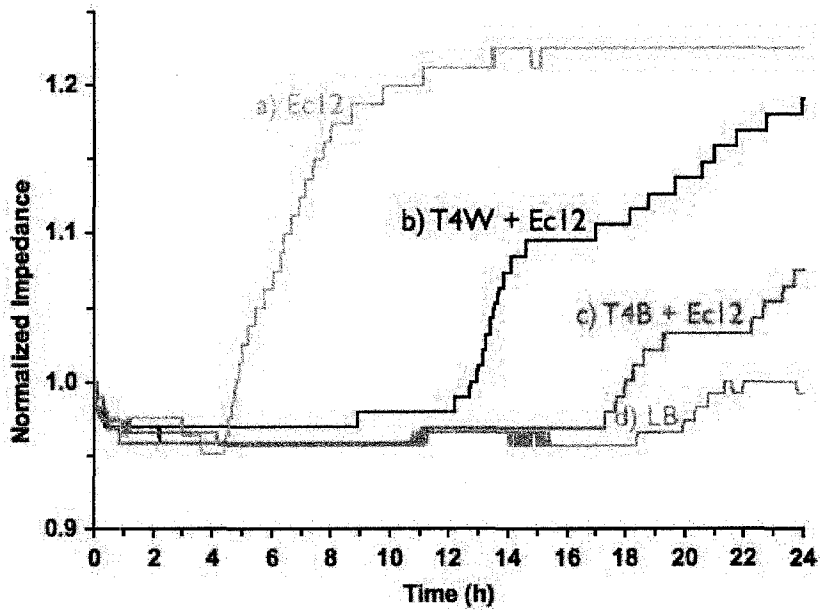

Figure 4.7: ECIS measurement from the growth of *E. coli* on 4 differently terminated gold electrodes functionalized with Sulfo-NHS-SS-Biotin and Streptavidin. a) Growth of *E. coli* without prior attachment of bacteriophage. This shows a normal bacterial growth curve rising at 4.5 h and peaking at 14 h. b) wild type phage (T4W) shows a 13 h delay in bacterial growth c) biotinylated phage (T4B) shows a 17.2 h delay in bacterial growth d) LB negative control shows a flat line until 18 h.

Figure 4.7 shows the measured impedance caused by the growth of the *E. coli* host in the presence of phage immobilized onto the gold electrodes. Trace a) corresponds to the growth of *E. coli* in the presence of streptavidin-terminated gold electrodes without any immobilization of phage. Trace b) corresponds to the bacterial growth in the presence of streptavidin-terminated gold electrodes with immobilized wild type T4 phage (T4W). Trace c) corresponds to the growth in the presence of streptavidin-terminated gold electrodes with immobilized biotinylated T4 phage (T4B). Trace d) corresponds to a well with streptavidin-terminated gold electrodes and filled with LB solution without any *E. coli* growth, thus providing a background control for comparison purposes. At the early stages of the

incubation (*i.e.* first four hours on Traces a) b) and c)), there was limited bacterial growth on the electrodes and in the solution and the impedance remained constant. After 4 to 18 h of incubation, depending on the preconditioning of the surface a) without phage, b) with T4W phage, and c) with T4B phage), an increase in the impedance signal is detected, indicating that the growth rate of bacteria on the surface and in the solution was not the same in all the samples. The devices devoid of any immobilized phage began to show measurable growth at 4.5 hours (trace a). This is a typical time for detecting an *E. coli* concentration of 10^4 cfu/mL as used in this experiment. In comparison, the devices onto which wild type phage were immobilized began to show growth after 13 h (trace b). This indicates that there were phage adsorbed non-specifically to the surface that desorb with time and could lyse and destroy a portion of the bacteria, thus delaying the detection of bacterial growth. Interestingly, the devices onto which biotinylated phage are immobilized begin to show growth after 17.2 h (trace c).

This greater delay indicates that the electrodes with the biotinylated phage delayed the growth of the bacteria in a more efficient manner, indicating that more phage were present on the surface. As was observed in the control surfaces (Figure 4.5a and b), the biotinylated phage T4B indeed attaches more specifically and in greater numbers to the streptavidin-terminated surface than the wild-type phage. This larger amount of phage on the initial surface resulted in a greater number of lysed bacteria and therefore in a larger number of phage released in solution during the initial hours of the incubation. This initially larger amount of phage in the system therefore further delayed the onset of bacteria growth both on the surface of the electrode and in the solution itself. This difference in bacterial growth delay could alternatively be explained by a difference of burst or latent time of the biotinylated phage compared to the wild type. However, we do not believe this to be the case as such genetic biotinylation has not been found to affect the viral activity of the T4 bacteriophage [141]. As was observed in Figure 4.5, the functionalization scheme of biotin-SAM and streptavidin therefore improved the binding of biotinylated phage onto the electrode surface, and delayed bacterial growth with greater efficiency than for devices that were initially treated with non-biotinylated phage.

4.5 Conclusion

We reported the streptavidin-mediated attachment of biotinylated phage onto gold electrodes, as well as the employment of such an attachment in an impedance biosensing system. The functionalization of gold surfaces with a biotin-terminated alkyl chain optimizes the attachment of streptavidin while minimizing the non-specific adsorption of the host *E. coli* These streptavidin-fuctionalized surfaces were then used to capture bacteriophage with biotinylated capsid heads. The capture efficiency of these surfaces was 5 times higher when exposed to biotinylated phage instead of the wild type ones. This indicates that the usage of biotin-streptavidin interaction chemistry significantly improves the attachment of the viruses onto the gold surfaces. These streptavidin modified surfaces were then used to mediate the attachment of biotinylated phage onto an impedance biosensing device. Such procedure significantly delayed the growth of the host bacteria, indicating that phage were efficiently bound to the functionalized surface. Devices onto which biotinlyated phage have been bound showed a greater delay in the growth of bacteria compared to devices onto which wild type phage were employed. This again indicated the improved efficiency of the attachment of the biotinylated phage in the presence of streptavidin-terminated gold. Such a chemical attachment of phage onto sensor surfaces could therefore be leveraged in numerous higly-sensitive sensing transduction platforms such as SPR, QCM, and microcantilevers, and enable the design of highly sensitive and highly specific platforms for the detection and identification of pathogenic microorganisms.

5

Bacteriophage Functionalized Cantilevers

The chemical attachment of T4 bacteriophage developed in the previous chapter was shown to provide a fivefold improvement in binding density compared to the physisorption of wild type bacteriophage. However, regions of the surface that are not covered by T4 bacteriophage are still susceptible to non-specific binding of bacteria. To further minimize this non-specific binding, a chemical immobilization procedure that utilizes the excellent non-fouling abilities of bovine serum albumin was developed.

This bacteriophage immobilization was prepared by attaching biotinylated T4 bacteriophage to a composite surface of streptavidin and biotinylated bovine serum albumin (BBSA). This surface was used to minimize the non-specific binding of bacteria while still exhibiting excellent adsorption of bacteriophage. The density of this immobilized surface was evaluated using electron microscopy. Densities of immobilized phage of 5 to 10 bacteriophage/100μm^2 were achieved, which is comparable to the first immobilization procedure.

The selectivity of bacterial adsorption on the T4 bacteriophage immobilized surface was then characterized. The surface was incubated with fluorescently labeled bacteria yielding a surface with specifically bound bacteria at densities as high as 60 cells/μm^2. Decreasing the concentration of phage used for immobilization was also found to decrease the number

of specifically bound bacteria to the surface.

Three different bacterial strains of *E. coli* were used to demonstrated the specificity of the phage immobilized surface. The bacteria were chosen as strains that are not lysed by bacteriophage T4. The non-specific binding of these three control strains yielded a density of 1 cell/100μm^2; an order of magnitude lower than the host strain. This additionally shows that a bacteriophage terminated surface can be used to differentiate between strains within a same bacterial species, a feat not possible by less specific antibodies.

This chemistry was applied to micro-cantilevers. Separate cantilevers were treated in host bacteria or non-host bacteria. The resonance shift due to host *E. coli* was shown to be an order of magnitude larger than the shift caused by the non-specific binding of bacteria. The results were confirmed by scanning electron micrographs showing the larger specific binding of host *E. coli* bacteria.

5.1 Materials

The preparation of buffers, culture and labeling of bacteria and bacteriophage amplification were prepared the same as the last section.

1-Octadecanethiol was purchased from Sigma Aldrich (Cat# 516678) and 1 mM solutions were prepared in ethanol. Biotinylated bovine serum albumin (BBSA) was purchased from Pierce (Cat#29130) and prepared at a concentration of 2 mg/mL in PBS. Streptavidin was obtained from Pierce (Cat# 21724), and the protein concentration was adjusted to 0.05 mg/mL in PBS. The millong buffer employed for substrate rinsing was prepared by mixing $NaH_2PO_4.H_20$ 1.8 g, $Na_2HPO_4.7H_2O$ 23.25 g, NaCl 5 g and 1000 mL of distilled water. Osmium tetroxide was obtained from Sigma Aldrich (O5500). A 5% TSBT solution was prepared by adding 25 μL of Tween20 to 5 mL of 5% TSB. Tap300GD gold coated AFM cantilevers were purchased from budget sensors. 0.05% PBST solution was prepared by adding 25 μL of Tween20 to 500 mL of PBS.

5.2 BBSA Bacteriophage Immobilization Chemistry

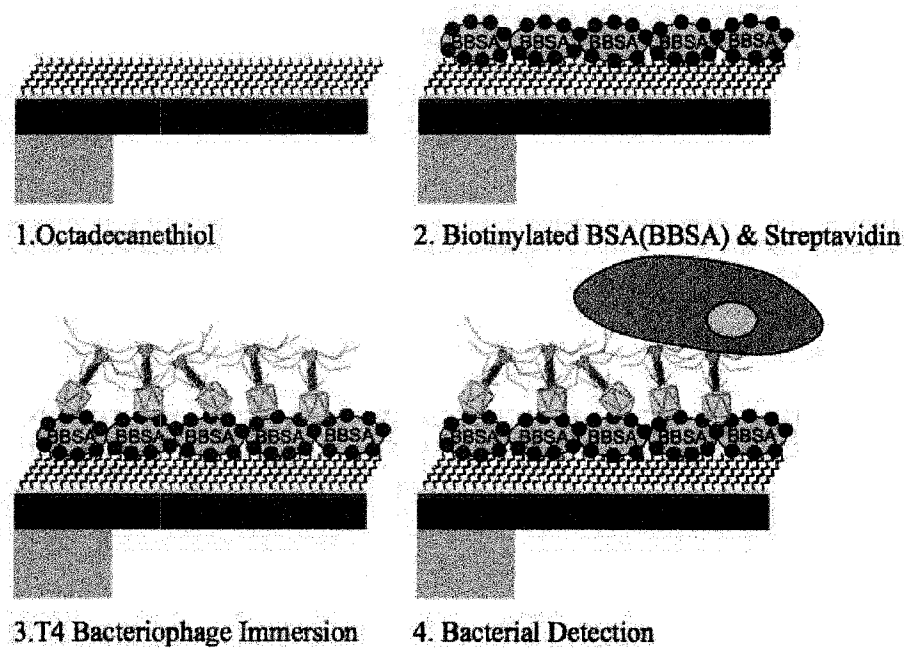

Figure 5.1: T4B immobilization procedure and bacterial detection

The T4 bacteriophage immobilization procedure is shown in figure 5.1. This immobilization chemistry was used both on regular surfaces and cantilevers. To characterize the bacteriophage and bacteria binding efficiency, experiments were undertaken on 5x5 mm silicon (111) chips sputter-coated with 5 nm of a chrome adhesion layer followed by 50 nm of gold. The chips were cleaned in piranha solution (2 sulfuric acid:1 hydrogen peroxide) for 10 min., and UV ozone cleaned for 1 h at 100°C. Samples were then rinsed in ethanol and dipped into 1 mM solution of hydrophobic 1-octadecanethiol for 1h on a rotating shaker. The samples were then rinsed three times in ethanol for 5 min. each rinse. Following two short rinses in PBS, the chips were immersed in biotinylated bovine serum albumin (BBSA) that binds to the 1-octadecanethiol for 30 min. on a rotating shaker. Following two short rinses in PBS, the chips were immersed into streptavidin that binds to the biotin groups of the BBSA for 15 min. on a rotating shaker. After two short rinses in PBS and lambda buffer, the chips were then immersed in a T4 bacteriophage solution ranging from 10^8 to 10^{11} pfu/mL in lambda buffer overnight

on a rotating shaker. Biotin on the T4 capsid binds to the streptavidin and immobilizes the bacteriophage on the surface.

5.3 Scanning Electron Microscopy Visualization

Phages are relatively electron transparent. To make phage easier to visualize in the SEM they can be made more electron opaque by fixing with glutaraldehyde and staining with a heavy compound such as OsO_4. Surfaces that were covered with 10^{11} pfu/mL phage solution were fixed with 1% glutaraldehyde (25 % aqueous solution) prepared with millong buffer. Fixation was done for 20 min. followed by 3 rinses in millong buffer for 5 min. The substrates were then incubated in 1% OsO_4 in millong buffer for 20 min. under gentle agitation. After rinsing twice with MilliQ water, the samples were immersed for 30 min. in tannic acid at 5 mg/mL in distilled water. Following another water rinse, 20 min. incubation in 1% OsO_4 was performed. Ethanol based dehydration was finally performed, which involved successive 5 min. immersions of the sample in 50%, 70%, 90% of ethanol mixed with water, followed by three immersions in 100% ethanol. Then samples were dried by using critical point drying technique and transfered to the high resolution field emission SEM (Hitachi S-4800).

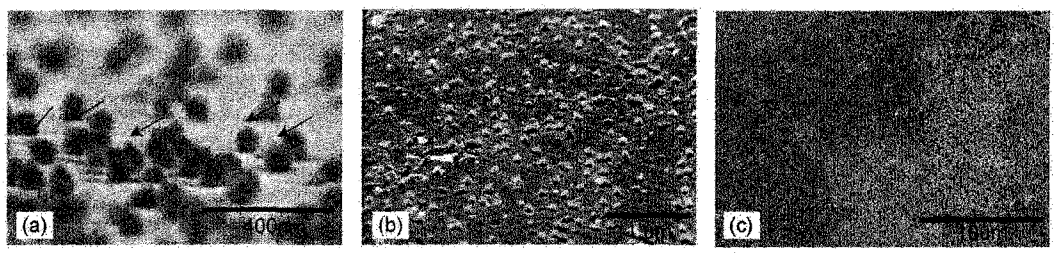

Figure 5.2: SEM of immobilized bacteriophage. a) and b) Tilted view SEM image of immobilized phage c) top view of the surface at a lower magnification

Tilted-view SEM images are shown in figure 5.2 a) and b). Figure 5.2 c) shows a top view at a lower magnification that was used to measure density. Phages can be seen as dark spots on a bright gold surface. The average density of immobilized phage was counted to be 5 to 10 phage/μm^2. This is a similar density to the first proposed immobilization

procedure from the the previous chapter. This similar density should therefore lead to a similar bacterial capture ability of the phage functionalized surface.

5.4 Bacterial Adsorption and Fluorescence Imaging

Bacterial adsorption was performed by dipping the surfaces with freshly immobilized phage into 5% TSB solution of SITO BC fluorescently labeled bacteria at 10^8 cfu/mL for 30 min. The substrates were then rinsed twice with 1 mL of 5% TSBT for 5 min. on an orbital shaker, then rinsed again for 5 min. in 5% TSB. Fluorescence imaging was performed similarly to the previous chapter. Briefly, an Olympus IX81 equipped with Roper Scientific CoolSnaps HQ CCD camera (Duluth, Georgia, U.S.A) was used. The sample was placed in a fluid cell made of a microscope slide and a mini transparent chamber. 300 μL of 5% TSB was added to prevent sample dehydration during fluorescence microscopy observation.

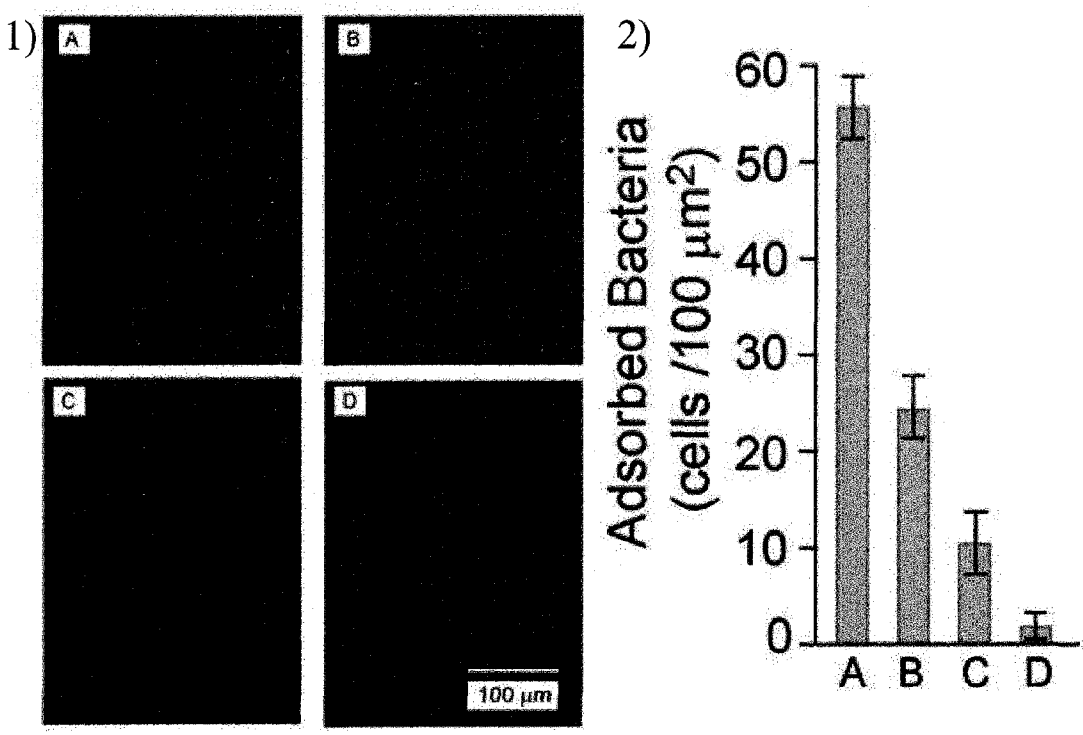

Figure 5.3: 1) Fluorescent microscope images of bacteria adsorbed on phage immobilized surface. Samples A, B, C and D are prepared with phage suspension of 10^{11} , 10^{10}, 10^9 and 10^8 pfu/mL respectively. 2) Quantification of adsorbed bacteria with samples prepared by using different concentration of phage suspension.

The interaction of phage immobilized surfaces with fluorescently labeled bacteria was measured by varying the concentration of phage used in the functionalization procedure. Figure 5.3 shows four surfaces that are functionalized with phage in concentrations of 10^{11} (A), 10^{10}(B), 10^{9} (C) and 10^{8} (D) pfu/mL. The specific adsorption of bacteria to the surface results in a proportional decrease of the number of adsorbed bacteria with the concentration of phage used in the immobilization procedure.

The bacterial density counts are graphed in figure 5.3. Samples A, B and C yield bacterial adsorption densities of 55±5, 25±5 and 11±2 cells/100μm^2 respectively. Meanwhile, sample D shows a bacterial adsorption level of less than 5 cells/100μm^2; this is of the same order of magnitude as surfaces with non-specific binding of bacteria. This indicates that coating surface with a phage solution greater than 10^{8} pfu/mL is needed to provide an advantage in specific binding of bacteria as compared to simple phage physisorption.

The 10^{11} pfu/mL phage immobilized surface was tested for specific bacterial adsorption by using four different strains of *E. coli* bacteria, including the host and three negative control strains which cannot be lysed by the T4 bacteriophage. Figure 5.4 shows fluorescent images of the phage immobilized surfaces after interaction with the different bacterial cultures. The bacterial densities plotted in the graph show that the target bacterial strain results in an average bacterial adsorption density of 55±5 cells/100μm^2. Meanwhile, the negative control surfaces using bacterial strains that are not lysed by the T4 phage (*PF*, *NP10*, *6M1N1*) show adsorption densities below 1 cell/100μm^2. It can be concluded that the phage immobilized surface promotes the specific binding of the target bacteria while exhibiting low non-specific binding of non-target bacteria that are not lysed by the immobilized bacteriophage.

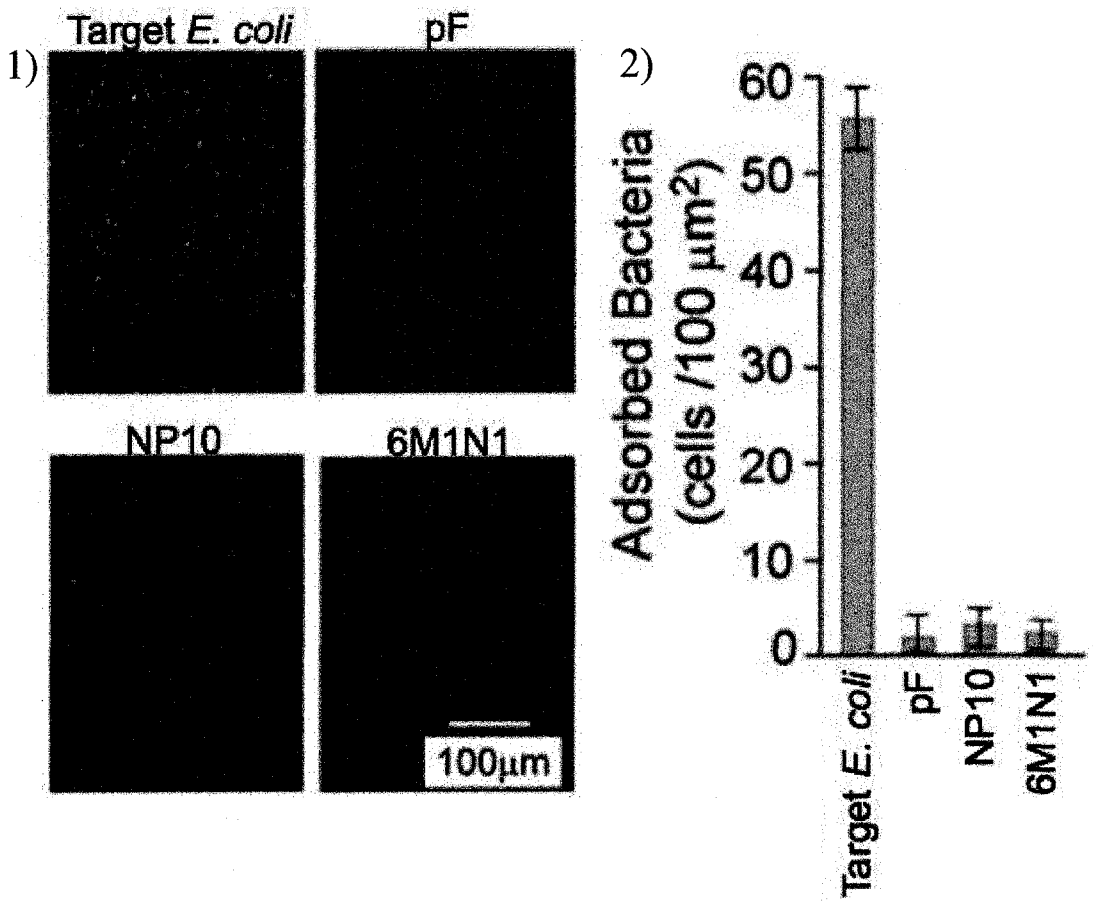

Figure 5.4: 1) Characterization of specific bacterial adsorption on phage immobilized surface (Sample A) using host and non-host bacteria (*PF*, *NP10* and *6M1N1*). 2) Quantification of specific adsorption

5.5 T4 Bacteriophage Functionalized Micro-Cantilevers.

The cantilevers used are silicon AFM cantilevers with 70 nm of gold coating. The length of the cantilevers is 125 μm $\pm$10 μm, width is 30 μm $\pm$5 μm and thickness is 4 μm $\pm$1 μm. The cantilevers natural resonant frequency is 300khz $\pm$100khz. The force constant is 40 N/m and can vary in a range from 20 N/m to 75 N/m. The bare unfunctionalized cantilevers are shown in figure 5.5. Cantilevers were resonated after three 5 min. rinses in Ethanol, a quick rinse in MilliQ water and nitrogen drying.

The functionalization procedure used on surfaces was used similarly on micro-cantilevers. After phage functionalization, the cantilevers were treated in bacterial solution

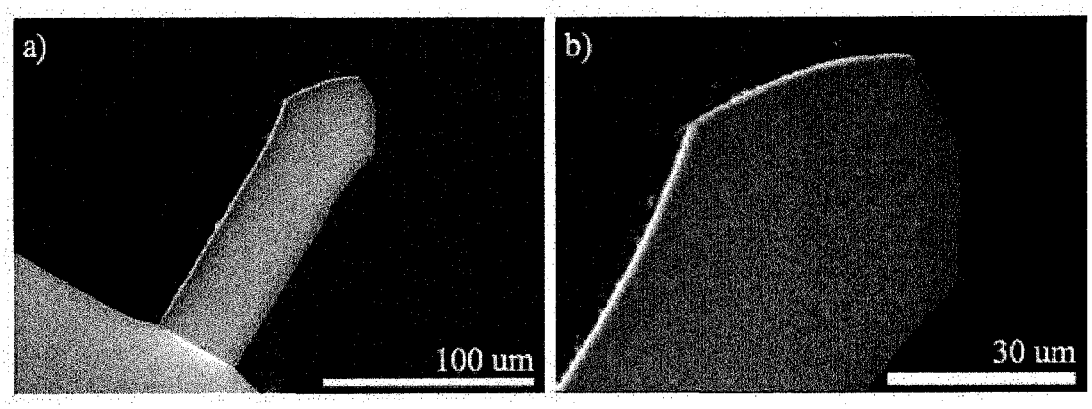

Figure 5.5: a) SEM of a bare unfunctionalized cantilever b) close up view of the cantilever

diluted in PBS buffer at a concentration of 10^8cfu/mL for 30 min. on a rotating shaker. The cantilevers were rinsed for 30 min. in PBST, followed by a quick rinse in PBS, MilliQ water and nitrogen drying. Then resonance measurements were taken using the tuning function of a Digital Instrument Dimension 3100 AFM (Santa-Clara, Ca, USA).

Two cantilevers were resonated after being treated with *E. coli* bacterial solution. The resonance graph or the first cantilever is shown in figure 5.6. Shifts of 2.874 kHz and 1.705 kHz were obtained for cantilevers 1 and 2 respectively.

Figure 5.7 shows SEM images of the cantilever. Dense specifically bound *E. coli* covers the surface and confirms the observed resonance shift. A resonance shift can be used to calculate the change in mass on the cantilever [58]:

$$\Delta m = \frac{k}{4n\pi^2}\left(\frac{1}{f_1^2} - \frac{1}{f_0^2}\right) \tag{5.1}$$

with k, the spring constant of the cantilever, f_0 the unloaded resonant frequency before functionalization, f_1 the resonant frequency after mass addition. We assume that the mass is uniformly distributed across the cantilever and use $n \approx 0.24$. We assume that the spring constant does not change after mass is added to the cantilever. Furthermore, we assume that the mass change is caused by adsorption to the functionalized side of the cantilever and that the silicon side of the cantilever is relatively free of non-specific binding.

The dry mass of bacteria is about 85 fg [58]. According to equation 5.1, the frequency shift of 2.874 kHz of the first cantilever corresponds to a change in mass of 1.31 pg. This

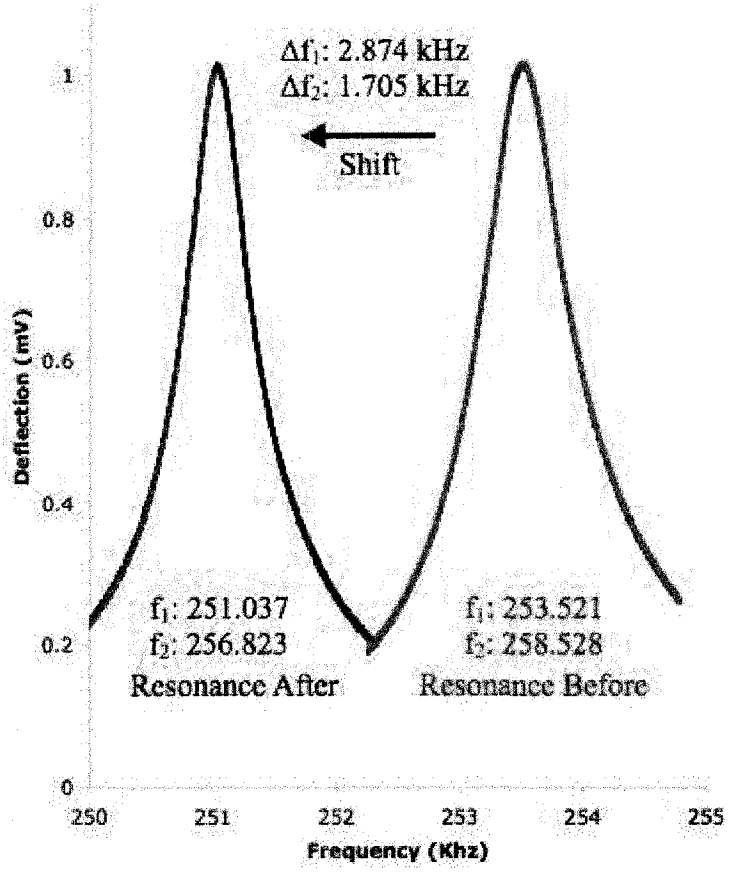

Figure 5.6: Resonance graph of a T4 bacteriophage functionalized cantilever (f_1) detecting specific binding of *E. coli* and resonance measurements of a second cantilever (f_2).

corresponds to a mass of approximately 15 bacterial cells. The second cantilever resulted in a shift of 1.705khz corresponding to a change in mass of 0.8 pg. The number of bacteria can be estimated to be 10 bacterial cells.

SEM images of the first cantilever is shown in figure 5.7. Specifically bound *E. coli* covers most of the surface. The cells are present in many layers and not easily countable, however there are certainly more than 15 bacteria by a few orders of magnitude. The fluorescence images yielded a density of about 55 cells/100 μm^2. On a cantilever that is about 125 μm long and 30 μm wide, we would expect to have about 2000 cells on the surface. The frequency shift would have been expected to be much larger due to such a dense adsorption of bacteria. However, the resonance shift is not only caused by the adsorption of bacteria but also by the functionalization layers. The self-assembled

mononolayer, BBSA and SA form a uniform film on the surface of the cantilever that is known to cause tensile stress and increase the resonance frequency. Additionally, *E. coli* bacteria is know to produce large quantities of biotin. The biotin binding to the streptavidin on the cantilever can create additional surface stress that increases the resonant frequency. These increases in resonance frequency coupled with the decrease in resonance frequency caused by the added mass of the monolayers and the *E. coli* result in a smaller total resonance shift.

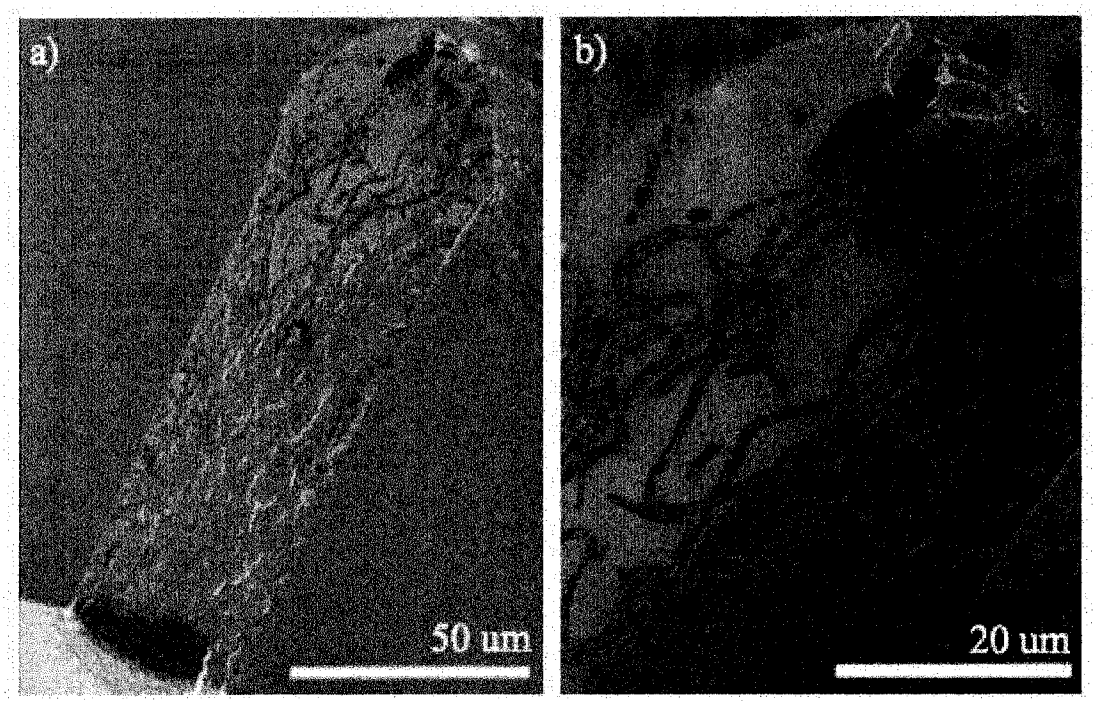

Figure 5.7: a) SEM showing specific binding of *E. coli* to T4 functionalized cantilever 1 b) close up view of the cantilever

Bacterial strain *6M1N1* was chosen as a negative control strain because of its inability to be lysed by T4 bacteriophage and hence cannot bind to the functionalized surface as shown in the bacterial adsorption experiments. A cantilever was functionalized and exposed to *6M1N1* bacterial solution. The resonance measurement are shown in figure 5.8. Three cantilevers were used in this experiment. The resonance shifts observed were 0.213 kHz (cantilever 1), 0.325 kHz (cantilever 2) and 0.219 kHz (cantilever 3). This shift is an order of magnitude smaller than the observed shift from the specific binding of *E. coli*.

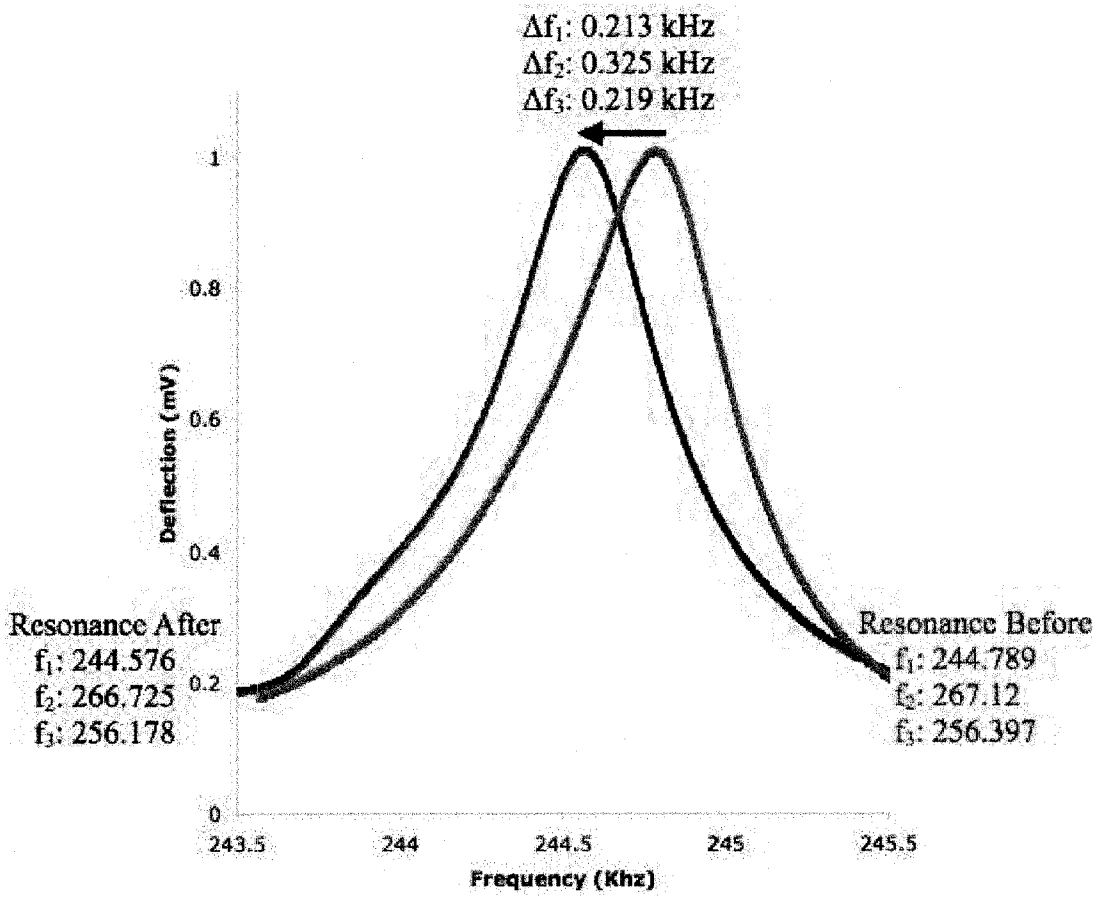

Figure 5.8: Negative control resonance measurements of non-specific binding of 61M1N1 bacteria to a T4B functionalized cantilever. Three cantilevers were measured (f_1, f_2, f_3)

SEM images of cantilever 1 are shown in figure 5.9. The non-specific binding of a few bacteria is observable on the cantilever surface. The few *6M1N1* bacteria adsorbed to the surface confirm the small observed resonance shift.

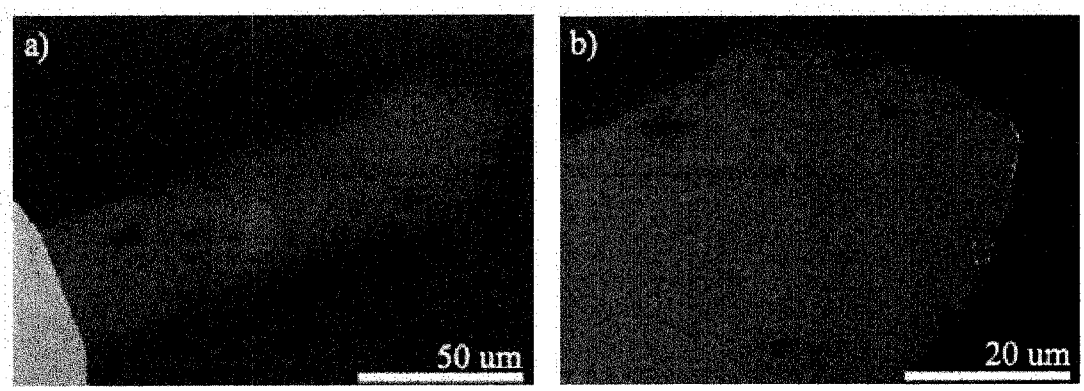

Figure 5.9: a) SEM showing non-specific binding of *6M1N1* to T4B functionalized cantilever 1 b) close up view of the cantilever

A final negative control was performed to verify to verify that the T4B was really responsible for the specific binding of *E. coli* to the cantilever surface. Three cantilevers were functionalized with 1-Octadecanethiol, BBSA and SA but were not treated in T4B. The cantilevers were exposed to *E. coli* similarly to the previous experiments and resonated. The resonance graph is shown in figure 5.10. Resonance shifts of 0.339 kHz (cantilever 1), 0.232 kHz (cantilever 2) and 0.117 kHz (cantilever 3) were observed. This shift is caused by the non-specific binding of *E. coli* to the cantilever surface is comparable to the shift caused by the non-specific binding of *6M1N1*.

SEM images of cantilever 3 are shown in figure 5.11. A few non-specificaly bound *E. coli* cells can be observed on the surface confirming the small resonance shift.

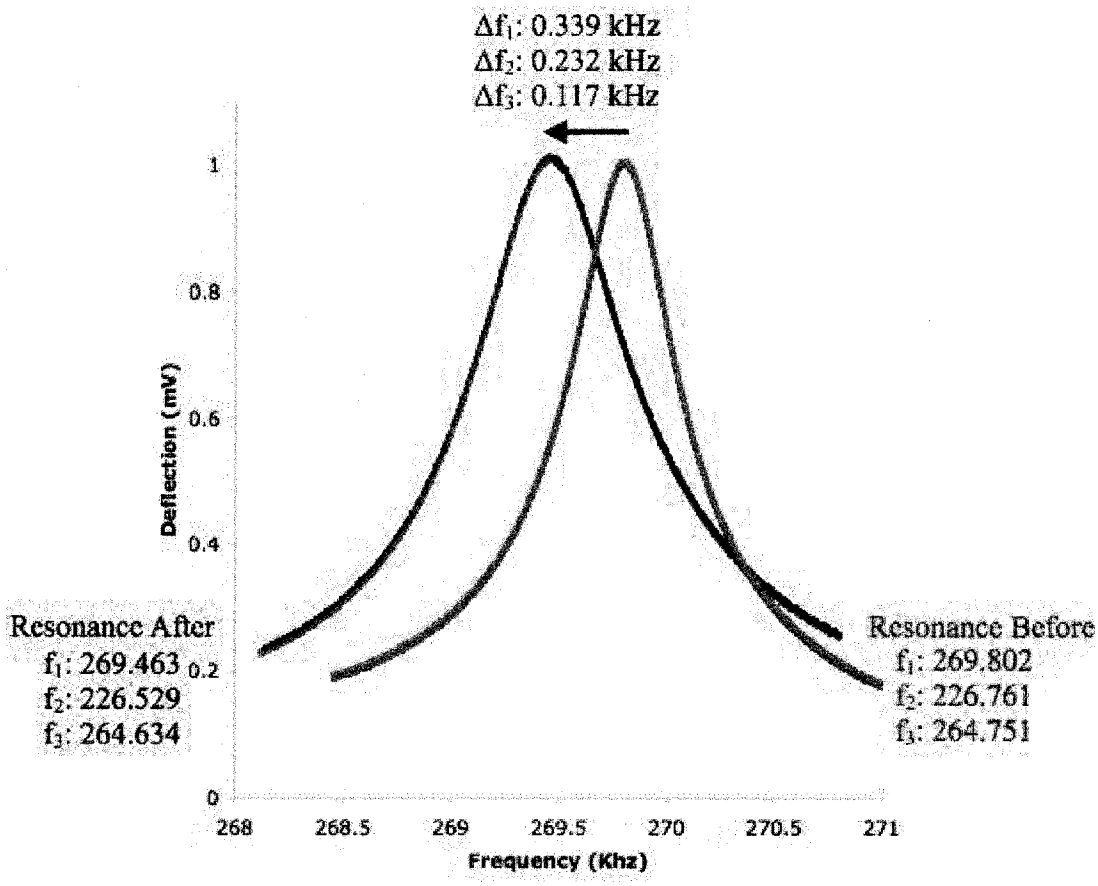

Figure 5.10: Negative control resonance measurements of non-specific binding of *E. coli* bacteria to a functionalized cantilever without T4B. Three cantilevers were measured (f_1, f_2, f_3)

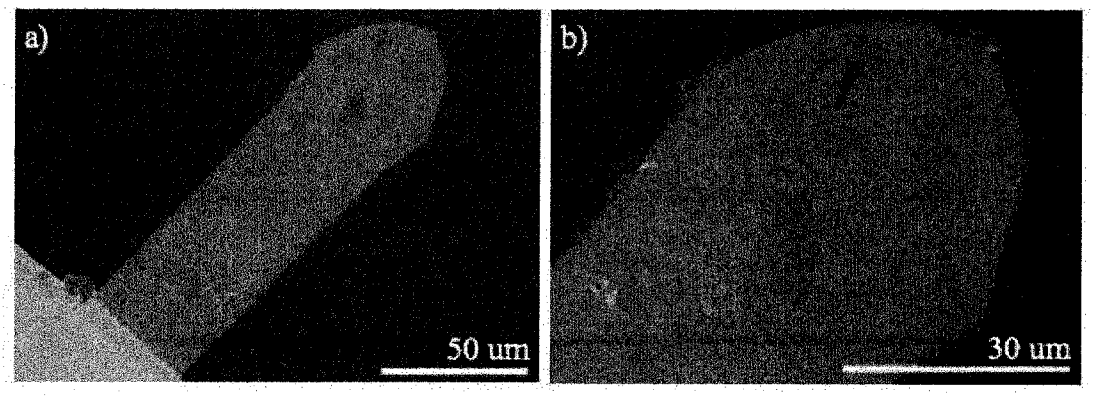

Figure 5.11: a) SEM showing non-specific binding of *E. coli* to functionalized cantilever 3 without T4B b) close up view of the cantilever

5.6 Conclusion

A T4 phage functionalization chemistry that minimizes the non-specific binding of bacteria was developed. Phages in suspension of 10^{11} pfu/mL were used for immobilzation to obtain a maximum phage density of 5 to 10 phage/μm^2. Specific bacterial adsorption was shown to occur at a density of 55 cells/100 μm^2. Non-specific binding of three *E. coli* strains that are not lysed by T4B was shown to occur at a density of 1 cell/100 μm^2. Thus, the selective adsorption of bacterial cells happens only in strains which can be lyzed by the immobilized phage.

Cantilevers were functionalized with T4 phage and resonated to detect the target *E. coli* strain. This resulted in a large frequency shift that was confirmed by observing the SEM images of the cantilevers showing abundant specifically bound *E. coli* cells. The negative controls of T4B functionalized cantilevers with non-specifically bound *6M1N1* bacteria, and functionalized cantilevers without immobilized T4B with non-specifically bound *E. coli* showed an order of magnitude decrease in resonance shift. This confirms the resonant detection of *E. coli* by T4B functionalized microcantilevers.

6 Conclusions

6.1 Summary

This work is the first time bacteriophage are immobilized and used as recognition probes on a micro-fabricated sensor. The chemical immobilization of bacteriophage onto cantilevers enables the highly specific detection of *EC12 E. coli*. The high specificity of bacteriophage is leveraged to differentiate between different strains of *E. coli*.

Genetically biotinylated T4 bacteriophage have been successfully immobilized onto the gold surfaces of biosensors. A biotin terminated SAM was used to bind streptavidin and efficiently immobilize T4 bacteriophage while minimizing non-specific binding of bacteria. The attached T4 bacteriophage yielded a density of 5 to 10 phage/μm^2; a five fold increase over simple physisorption.

This chemical immobilization of T4 bacteriophage was shown to affect the growth of bacteria in an ECIS sensor. It was found that the T4B functionalized surface significantly delays the growth of the host bacteria by up to 17.2 h. The non-specific binding of wild type phage onto the streptavidin surface was found to be less efficient and cause a lesser growth delay of 13 h.

A second T4 phage functionalization chemistry was developed to further minimizes non-

specific binding. Similar phage densities of 5 to 10 phage/μm^2 were obtained. The specific binding of bacteria was found to occur at a density of 55 cells/100 μm^2 and the non-specific binding of three *E. coli* strains that are not lysed by T4B was shown to occur at a density of 1 cell/100 μm^2. Selective adsorption of bacteria was shown to happen only in strains which can be lysed by the immobilized phage.

T4 functionalized cantilevers were resonated to detect the target *E. coli* strain. Frequency shifts were confirmed by observing SEM images of the cantilevers showing abundant specifically bound *E. coli* cells. Negative controls of T4B functionalized cantilevers with non-specifically bound 6M1N1 bacteria, and functionalized cantilevers without immobilized T4B with non-specifically bound *E. coli* showed an order of magnitude decrease in resonance shift confirming the resonant detection of *E. coli* by T4B functionalized microcantilevers.

6.2 Recommendations for Future Work

This work can be improved in several ways. Streptavidin was used in all the experiments. Neutravidin is known to have lower non-specific binding than Streptavidin. It would therefore be advantageous and straightforward to convert all the T4 functionalization procedures developed to use Neutravidin.

The cantilevers that were used during the experiments were not optimal for *E. coli* bacterial detection. Smaller cantilevers with higher quality factors and higher resonant frequencies would be ideal. Resonance measurements could also be taken in vacuum instead of air to reduce damping and improve the quality factor. Lower concentrations of bacteria could be used to quantify the minimal detection limit and compare with other biosensors such as QCM and SPR.

It is known that the high specificity of bacteriophage to bacteria is due to the recognition and binding of the tail fibers and base plate. It would be feasible to isolate the bacteriophage tail and base plate proteins and to immobilize then onto cantilever surfaces, forgoing the need of complete phage. A dense monolayer of these proteins could potentially leads to denser and more efficient specific binding of bacteria.

Bibliography

[1] W. E. C. Moore and L. V. Holdeman, "Human fecal flora - normal flora of 20 japanese-hawaiins," *Applied Microbiology*, vol. 27, no. 5, pp. 961–979, 1974.

[2] J. H. Cummings and G. T. Macfarlane, "The control and consequences of bacterial fermentation in the human colon," *Journal of Applied Bacteriology*, vol. 70, pp. 443–459, Jun 1991.

[3] R. Duchmann, I. Kaiser, E. Hermann, W. Mayet, K. Ewe, and K. H. M. ZumBuschenfelde, "Tolerance exists towards resident intestinal flora but is broken in active inflammatory bowel disease (ibd)," *Clinical and Experimental Immunology*, vol. 102, pp. 448–455, Dec 1995.

[4] L. V. Hooper, M. H. Wong, A. Thelin, L. Hansson, P. C. Falk, and J. I. Gordon, "Molecular analysis of commensal host-microbial relations hips in the intestine," *Science*, vol. 291, pp. 881–884, Feb 2001.

[5] M. J. Jedrzejas, "Pneumococcal virulence factors: Structure and function," *Microbiology and Molecular Biology Reviews*, vol. 65, pp. 187–+, Jun 2001.

[6] M. van Deuren, P. Brandtzaeg, and J. W. M. van der Meer, "Update on meningococcal disease with emphasis on pathogenesis and clinical management," *Clinical Microbiology Reviews*, vol. 13, pp. 144–+, Jan 2000.

[7] S. Nakano, A. Matsumura, and T. Yamada, "A pcr assay for detection of acetic acid-tolerant lactic acid bacteria in acidic food products," *J. Food. Prot.*, vol. 67, pp. 610–615, 2004.

[8] A. I. Mata, A. Gibello, A. Casamayor, M. M. Blanco, L. Domínguez, and J. F. Fernandez-Garayzabal, "Multiplex pcr assay for detection of bacterial pathogens associated with warm-water streptococcosis in fish," *Appl. Environ. Microb.*, vol. 70, pp. 3183–3187, 2004.

[9] K. Janyapoon, S. Korbsrisate, H. Thamapa, S. Thongmin, S. Kanjanahareutai, N. Wongpredee, and S. Sarasombath, "Rapid detection of salmonella enterica serovar choleraesuis in blood cultures by a dot blot enzyme-linked immunosorbent assay," *Clin. Diagn. Lab. Immun.*, vol. 7, pp. 977–979, 2000.

[10] Y. Hong, M. E. Berrang, T. Liu, C. L. Hofacre, S. Sanchez, L. Wang, and J. J. Maurer, "Rapid detection of campylobacter coli, c. jejuni, and salmonella enterica on poultry carcasses by using pcr–enzyme-linked immunosorbent assay," *Appl. Environ. Microb.*, vol. 69, pp. 3492–3499, 2003.

[11] M. Jones, A. Fox, A. Barnes, B. Oppenheim, P. Balagopal, G. Morgenstern, and J. Scarffe, "Pcr-elisa for the early diagnosis of invasive pulmonary aspergillus infection in neutropenic patients," *J. Clin. Pathol.*, vol. 51, pp. 652–656, 1998.

[12] D. G. Myszka, M. Jonsen, and B. Graves, "Equilibrium analysis of high affinity interactions using biacore," *Analytical Biochemistry*, vol. 265, pp. 326–330, July 1998.

[13] J. Menlendez, R. Carr, D. Barholomew, H. Taneja, S. Yee, C. Jung, and C. Furlong, "Development of a surface plasmon resonance sensor for commercial applications," *Sensors and Actuators B-Chemical*, vol. 38-39, pp. 375–379, 1997.

[14] J. Homola, J. Dostalek, S. F. Chen, A. Rasooly, S. Y. Jiang, and S. S. Yee, "Spectral surface plasmon resonance biosensor for detection of staphylococcal enterotoxin b in milk," *International Journal of food microbiology*, vol. 75, pp. 61–69, May 2002.

[15] B. K. Oh, Y. K. Kim, Y. M. Bae, W. H. Lee, and J. W. Choi, "Detection of escherichia coli o157 : H7 using immunosensor based on surface plasmon resonance," *Journal of microbiology and biotechnology*, vol. 12, pp. 780–786, Oct 2002.

[16] J. Waswa, J. Irudayaraj, and C. DebRoy, "Direct detection of e-coli o157 : H7 in selected food systems by a surface plasmon resonance biosensor," *Lwt-Food science and technology*, vol. 40, no. 2, pp. 187–192, 2007.

[17] *Polymer Handbook*. No. 469 in VII, Wiley, third ed., September 1989.

[18] C. R.M., M. J.J., J. M.B., L. G.J., and G. G.G., "Quartz crystal microbalance detection of vibro cholerae o139 serotype," *Journal of Immunolology Methods*, vol. 187, pp. 121–125, 1995.

[19] E. Prusak-Sochaczewski and J. L. G. Guibault, "Development of piezoelectric immunosensor for the detection of salmonella typhimurium," *Enzyme Microbiology Technology*, vol. 12, pp. 173–177, 1990.

[20] M. Jacobs, R. Cater, G. Lubrano, and G. Guibault, "A piezoelectric biosensor for listeria-monocytogenes," *Am. Lab.*, vol. 27, no. 11, pp. 26–28, 1995.

[21] I. BenDov, I. Willner, and E. Zisman, "Piezoelectric immunosensors for urine specimens of chlamydia trachomatis employing quartz crystal microbalance microgravimetric analyses," *Analytical Chemistry*, vol. 69, pp. 3506–3512, Sep 1997.

[22] D. A. Borkholder, J. Bao, N. I. Maluf, E. R. Perl, and G. T. A. Kovacs, "Microelectrode arrays for stimulation of neural slice preparations," *Journal of Neuroscience Methods*, vol. 77, pp. 61–66, Nov 1997.

[23] A. A. Shulga, A. P. Soldatkin, A. V. Elskaya, S. V. Dzyadevich, S. V. Patskovsky, and V. I. Strikha, "Thin-film conductometric biosensors for glucose and urea determination," *Biosensors & Bioelectronics*, vol. 9, no. 3, pp. 217–223, 1994.

[24] A. Steinschaden, D. Adamovic, G. Jobst, R. Glatz, and G. Urban, "Miniaturised thin film conductometric biosensors with high dynamic range and high sensitivity," *Sensors and Actuators B-Chemical*, vol. 44, pp. 365–369, Oct 1997.

[25] H. Suzuki, H. Arakawa, and I. Karube, "Fabrication of a sensing module using micromachined biosensors," *Biosensors & Bioelectronics*, vol. 16, pp. 725–733, Dec 2001.

[26] S. Andreescu, A. Avramescu, C. Bala, V. Magearu, and J. L. Marty, "Detection of organophosphorus insecticides with immobilized acetylcholinesterase - comparative study of two enzyme sensors," *Analytical and Bioanalytical Chemistry*, vol. 374, pp. 39–45, Sep 2002.

[27] G. Marrazza, I. Chianella, and M. Mascini, "Disposable dna electrochemical sensor for hybridization detection," *Biosensors & Bioelectronics*, vol. 14, pp. 43–51, Jan 1999.

[28] T. G. Drummond, M. G. Hill, and J. K. Barton, "Electrochemical dna sensors," *Nature biotechnology*, vol. 21, pp. 1192–1199, Oct 2003.

[29] S. J. Park, T. A. Taton, and C. A. Mirkin, "Array-based electrical detection of dna with nanoparticle probes," *Science*, vol. 295, pp. 1503–1506, Feb 2002.

[30] "http://www.nanogen.com/," june 16, 2007.

[31] R. Gomez, R. Bashir, and A. K. Bhunia, "Microscale electronic detection of bacterial metabolism," *Sensors and Actuators B-Chemical*, vol. 86, pp. 198–208, Sep 2002.

[32] L. I. Netchiporouk, N. F. Shram, N. JaffrezicRenault, C. Martelet, and R. Cespuglio, "In vivo brain glucose measurements: Differential normal pulse voltammetry with enzyme-modified carbon fiber microelectrodes," *Analytical Chemistry*, vol. 68, pp. 4358–4364, Dec 1996.

[33] N. F. Shram, L. I. Netchiporouk, C. Martelet, N. JaffrezicRenault, and R. Cespuglio, "Brain glucose: Voltammetric determination in normal and hyperglycaemic rats using a glucose microsensor," *Neuroreport*, vol. 8, pp. 1109–1112, Mar 1997.

[34] R. Hintsche, B. Moller, I. Dransfeld, U. Wollenberger, F. Scheller, and B. Hoffmann, "Chip biosensors on thin-film metal electrodes," *Sensors and Actuators B-Chemical*, vol. 4, pp. 287–291, Jun 1991.

[35] R. Hintsche, C. Kruse, A. Uhlig, M. Paeschke, T. Lisec, U. Schnakenberg, and B. Wager, "Chemical microsensor systems for medical applications in catheters," *Sensors and Actuators B-Chemical*, vol. 27, pp. 471–473, Jun 1995.

[36] H. Zhu and M. Snyder, "Protein chip technology," *Current Opinion in Chemical Biology*, vol. 7, pp. 55–63, Feb 2003.

[37] S. Brahim, D. Narinesingh, and A. Guiseppi-Elie, "Polypyrrole-hydrogel composites for the construction of clinically important biosensors," *Biosensors & Bioelectronics*, vol. 17, pp. 53–59, Jan 2002.

[38] S. Brahim, D. Narinesingh, and A. Guiseppi-Elie, "Bio-smart hydrogels: co-joined molecular recognition and signal transduction in biosensor fabrication and drug delivery," *Biosensors & Bioelectronics*, vol. 17, pp. 973–981, Dec 2002.

[39] X. X. Cai, N. Klauke, A. Glidle, P. Cobbold, G. L. Smith, and J. M. Cooper, "Ultra-low-volume, real-time measurements of lactate from the single heart cell using microsystems technology," *Analytical Chemistry*, vol. 74, pp. 908–914, Feb 2002.

[40] C. J. Yu, Y. J. Wan, H. Yowanto, J. Li, C. L. Tao, M. D. James, C. L. Tan, G. F. Blackburn, and T. J. Meade, "Electronic detection of single-base mismatches in dna with ferrocene-modified probes," *Journal of the American Chemical Society*, vol. 123, pp. 11155–11161, Nov 2001.

[41] R. M. Umek, S. W. Lin, J. Vielmetter, R. H. Terbrueggen, B. Irvine, C. J. Yu, J. F. Kayyem, H. Yowanto, G. F. Blackburn, D. H. Farkas, and Y. P. Chen, "Electronic detection of nucleic acids - a versatile platform for molecular diagnostics," *Journal of Molecular Diagnostics*, vol. 3, pp. 74–84, May 2001.

[42] M. Barbaro, A. Bonfiglio, L. Raffo, A. Alessandrini, P. Facci, and I. Barak, "A cmos, fully integrated sensor for electronic detection of dna hybridization," *IEEE electron device letters*, vol. 27, pp. 595–597, Jul 2006.

[43] M. Barbaro, A. Bonfiglio, L. Raffo, A. Alessandrini, P. Facci, and I. Barak, "Fully electronic dna hybridization detection by a standard cmos biochip," *Sensors and Actuators B-Chemical*, vol. 118, pp. 41–46, Oct 2006.

[44] M. Schienle, C. Paulus, A. Frey, F. Hofmann, B. Holzapfl, P. Schindler-Bauer, and R. Thewes, "A fully electronic dna sensor with 128 positions and in-pixel a/d conversion," *IEEE journal of solid state circuits*, vol. 39, pp. 2438–2445, Dec 2004.

[45] U. Schnakenberg, T. Lisec, R. Hintsche, I. Kuna, A. Uhlig, and B. Wagner, "Novel potentiometric silicon sensor for medical devices," *Sensors and Actuators B-Chemical*, vol. 34, pp. 476–480, Aug 1996.

[46] M. Lehmann, W. Baumann, M. Brischwein, H. J. Gahle, I. Freund, R. Ehret, S. Drechsler, H. Palzer, M. Kleintges, U. Sieben, and B. Wolf, "Simultaneous measurement of cellular respiration and acidification with a single cmos isfet," *Biosensors & Bioelectronics*, vol. 16, pp. 195–203, May 2001.

[47] A. Fanigliulo, P. Accossato, M. Adami, M. Lanzi, S. Martinoia, S. Paddeu, M. T. Marodi, A. Rossi, M. Sartore, M. Grattarola, and C. Nicolini, "Comparison between a laps and an fet-based sensor for cell-metabolism detection," *Sensors and Actuators B-Chemical*, vol. 32, pp. 41–48, Apr 1996.

[48] P. Gavazzo, P., S. Paddeu, M. Sartote, and C. Nicolini, "Study of the relationship between extracellular acidification and cell viability by a silicon-based sensor," *Sensors and Actuators B-Chemical*, vol. 19, pp. 368–372, Apr 1994.

[49] A. Seki, K. Motoya, S. Watanabe, and I. Kubo, "Novel sensors for potassium, calcium and magnesium ions based on a silicon transducer as a light-addressable potentiometric sensor," *Analytica chimica acta*, vol. 382, pp. 131–136, Feb 1999.

[50] J. Fritz, E. B. Cooper, S. Gaudet, P. K. Sorger, and S. R. Manalis, "Electronic detection of dna by its intrinsic molecular charge," *Proceedings of the National Academy of Science of the United States of America*, vol. 99, pp. 14142–14146, Oct 2002.

[51] Y. Cui, Q. Q. Wei, H. K. Park, and C. M. Lieber, "Nanowire nanosensors for highly sensitive and selective detection of biological and chemical species," *Science*, vol. 293, pp. 1289–1292, Aug 2001.

[52] K. Besteman, J. O. Lee, F. G. M. Wiertz, H. A. Heering, and C. Dekker, "Enzyme-coated carbon nanotubes as single-molecule biosensors," *Nano Letters*, vol. 3, pp. 727–730, Jun 2003.

[53] B. Ilic, H. G. Craighead, S. Krylov, W. Senaratne, C. Ober, and P. Neuzil, "Attogram detection using nanoelectromechanical oscillators," *Journal of Applied Physics*, vol. 95, pp. 3694–3703, Apr 2004.

[54] N. V. Lavrik and P. G. Datskos, "Femtogram mass detection using photothermally actuated nanomechanical resonators," *Applied Physics Letters*, vol. 82, pp. 2697–2699, Apr 2003.

[55] T. D. Stowe, K. Yasumura, T. W. Kenny, D. Botkin, K. Wago, and D. Rugar, "Attonewton force detection using ultrathin silicon cantilevers," *Applied Physics Letters*, vol. 71, pp. 288–290, Jul 1997.

[56] R. Bashir, "Biomems: state-of-the-art in detection, opportunities and prospects," *Avanced Drug Delivery Reviews*, vol. 56, pp. 1565–1586, Sep 2004.

[57] B. Ilic, D. Czaplewski, M. Zalalutdinov, H. G. Craighead, P. Neuzil, C. Campagnolo, and C. Batt, "Single cell detection with micromechanical oscillators," *Journal of Vacuum Science & Technology B*, vol. 19, pp. 2825–2828, Nov-Dec 2001.

[58] A. Gupta, D. Akin, and R. Bashir, "Detection of bacterial cells and antibodies using surface micromachined thin silicon cantilever resonators," *Journal of Vacuum Science & Technology B*, vol. 22, no. 6, pp. 2785–2791, 2004.

[59] T. Thudat, G. Chen, R. Warmack, D. Allison, and E. Wachter, "Vapor detection using resonating microcantilevers," *Analytical Biochemistry*, vol. 67, pp. 519–521, 1995.

[60] T. Thundat, R. Warmack, G. Chen, and D. Allison], "Thermal and ambient-induced deflections of scanning force microscope cantilevers," *Applied Physics Letters*, pp. 2894–2896, 1994.

[61] D. Rugar, H. Mamin, R. Erlandsson, J. Stern, and B. Terris, "Force microscope using a fiber-optic displacement sensor," *Rev. Sci. Instrum.*, no. 59, pp. 2337–2340, 1988.

[62] N. Blanc, J. Brugger, N. de Rooij, and U. Duerig, "Scanning force microscopy in the dynamic mode using microfabricated capacitive sensors," *Journal of Vacuum Science & Technology B*, vol. 14, p. 901, 1996.

[63] M. Tortonese, R. Barett, and C. Quate, "Atomic resolution with an atomic force microscope using piezoresistive detection," *Applied Physics Letters*, pp. 834–836, 1993.

[64] R. Linnemann, T. Gotszalk, L. Hadjiski, and I. Rangelow, "Characterization of a cantilever with an integrated deflection sensor," *Thin Solid Films*, vol. 264, pp. 159–164, 1995.

[65] O. Hansen and A. Boisen, "Noise in piezoresistive atomic force microscopy," *Nanotechnology*, vol. 10, pp. 51–60, Mar 1999.

[66] P. A. Rasmussen, J. Thaysen, O. Hansen, S. C. Eriksen, and A. Boisen, "Optimised cantilever biosensor with piezoresistive read-out," *ULTRAMICROSCOPY*, vol. 97, pp. 371–376, Oct-Nov 2003.

[67] T. Akiyama, U. Staufer, N. F. de Rooij, D. Lange, C. Hagleitner, O. Brand, H. Baltes, A. Tonin, and H. R. Hidber, "Integrated atomic force microscopy array probe with metal-oxide-semiconductor field effect transistor stress sensor, thermal bimorph actuator, and on-chip complementary metal-oxide-semiconductor electronics," *Journal of Vacuum Science & Technology B*, vol. 18, pp. 2669–2675, Nov-Dec 2000.

[68] R. Raiteri, M. Grattarola, H. J. Butt, and P. Skladal, "Micromechanical cantilever-based biosensors," *Sensors and Actuators B-Chemical*, vol. 79, pp. 115–126, Oct 2001.

[69] R. Marie, J. Thaysen, C. B. V. Christensen, and A. Boisen, "A cantilever-based sensor for thermal cycling in buffer solution," *Microelectronic Engineering*, vol. 67-8, pp. 893–898, Jun 2003.

[70] J. Thaysen, A. D. Yalcinkaya, P. Vettiger, and A. Menon, "Polymer-based stress sensor with integrated readout," *Journal of physics D-applied physics*, vol. 35, pp. 2698–2703, Nov 2002.

[71] H. J. Butt, "A sensitive method to measure changes in the surface stress of solids," *Journal of Coloid and Interface Science*, vol. 180, pp. 251–260, Jun 1996.

[72] J. Fritz, M. K. Baller, H. P. Lang, T. Strunz, E. Meyer, H. J. Guntherodt, E. Delamarche, C. Gerber, and J. K. Gimzewski, "Stress at the solid-liquid interface of self-assembled monolayers on gold investigated with a nanomechanical sensor," *Langmuir*, vol. 16, pp. 9694–9696, Dec 2000.

[73] X. H. Xu, T. G. Thundat, G. M. Brown, and H. F. Ji, "Detection of hg2+ using microcantilever sensors," *Analytical Chemistry*, vol. 74, pp. 3611–3615, Aug 2002.

[74] H. F. Ji and T. Thundat, "In situ detection of calcium ions with chemically modified microcantilevers," *Biosensors & Bioelectronics*, vol. 17, pp. 337–343, Apr 2002.

[75] H. F. Ji, T. Thundat, R. Dabestani, G. M. Brown, P. F. Britt, and P. V. Bonnesen, "Ultrasensitive detection of cro42- using a microcantilever sensor," *Analytical Chemistry*, vol. 73, pp. 1572–1576, Apr 2001.

[76] S. Cherian, R. K. Gupta, B. C. Mullin, and T. Thundat, "Detection of heavy metal ions using protein-functionalized microcantilever sensors," *Biosensors & Bioelectronics*, vol. 19, pp. 411–416, Dec 2003.

[77] Y. M. Yang, H. F. Ji, and T. Thundat, "Nerve agents detection using a cu2+/l-cysteine bilayer-coated microcantilever," *Journal of American Chemical Society*, vol. 125, pp. 1124–1125, Feb 2003.

[78] T. Thundat, P. I. Oden, and R. J. Warmack, "Microcantilever sensors," *Microscale Thermophysical Engineering*, vol. 1, pp. 185–199, Jul-Sep 1997.

[79] C. Grogan, R. Raiteri, G. M. O'Connor, T. J. Glynn, V. Cunningham, M. Kane, M. Charlton, and D. Leech, "Characterisation of an antibody coated microcantilever as a potential immuno-based biosensor," *Biosensors & Bioelectronics*, vol. 17, pp. 201–207, Mar 2002.

[80] G. H. Wu, R. H. Datar, K. M. Hansen, T. Thundat, R. J. Cote, and A. Majumdar, "Bioassay of prostate-specific antigen (psa) using microcantilevers," *Nature biotechnology*, vol. 19, pp. 856–860, Sep 2001.

[81] R. Raiteri, G. Nelles, H. J. Butt, W. Knoll, and P. Skladal, "Sensing of biological substances based on the bending of microfabricated cantilevers," *Sensors and Actuators B-Chemical*, vol. 61, pp. 213–217, Dec 1999.

[82] R. Marie, H. Jensenius, J. Thaysen, C. B. Christensen, and A. Boisen, "Adsorption kinetics and mechanical properties of thiol-modified dna-oligos on gold investigated by microcantilever sensors," *Ultramicroscopy*, vol. 91, pp. 29–36, May 2002.

[83] J. Fritz, M. K. Baller, H. P. Lang, H. Rothuizen, P. Vettiger, E. Meyer, H. J. Guntherodt, C. Gerber, and J. K. Gimzewski, "Translating biomolecular recognition into nanomechanics," *Science*, vol. 288, pp. 316–318, Apr 2000.

[84] K. M. Hansen, H. F. Ji, G. H. Wu, R. Datar, R. Cote, A. Majumdar, and T. Thundat, "Cantilever-based optical deflection assay for discrimination of dna single-nucleotide mismatches," *Analytical Chemistry*, vol. 73, pp. 1567–1571, Apr 2001.

[85] S. Weigert, M. Dreier, and M. Hegner, "Frequency shifts of cantilevers vibrating in various media," *Applied Physics Letters*, vol. 69, pp. 2834–2836, Nov 1996.

[86] G. Y. Chen, R. J. Warmack, T. Thundat, D. P. Allison, and A. Huang, "Resonance responce of scanning force microscopy cantilevers," *Review of Scientific Instruments*, vol. 65, pp. 2532–2537, Aug 1994.

[87] A. Gupta, D. Akin, and R. Bashir, "Single virus particle mass detection using microresonators with nanoscale thickness," *Applied Physics Letters*, vol. 84, pp. 1976–1978, Mar 2004.

[88] D. Lange, C. Hagleitner, A. Hierlemann, O. Brand, and H. Baltes, "Complementary metal oxide semiconductor cantilever arrays on a single chip: Mass-sensitive detection of volatile organic compounds," *Analytical Chemistry*, vol. 74, pp. 3084–3095, Jul 2002.

[89] J. H. Lee, K. H. Yoon, K. S. Hwang, J. Park, S. Ahn, and T. S. Kim, "Label free novel electrical detection using micromachined pzt monolithic thin film cantilever for the detection of c-reactive protein," *Biosensors & Bioelectronics*, vol. 20, pp. 269–275, Sep 2004.

[90] J. H. Lee, K. S. Hwang, J. Park, K. H. Yoon, D. S. Yoon, and T. S. Kim, "Immunoassay of prostate-specific antigen (psa) using resonant frequency shift of piezoelectric nanomechanical microcantilever," *Biosensors & Bioelectronics*, vol. 20, pp. 2157–2162, Apr 2005.

[91] R. Hendrix, "Bacteriophages: evolution of the majority," *Theoretical Population Biology*, vol. 61, pp. 471–480, 2002.

[92] M. Pedulla, M. Ford, J. Houtz, T. Karthikeyan, C. Wadsworth, J. Lewis, D. Jacobs-Sera, J. Falbo, G. J., N. P. Brucker, W. Kumar, V. Kandasamy, J. Keenan, L., S. Bardarov, J. Kriakov, J. Lawrence, W. J. Jacobs, R. Hendrix, and G. Hatfull, "Origins of highly mosaic mycobacteriophage genomes," *Cell*, vol. Cell, pp. 171–182, 2003.

[93] F. D'Herelle, "Sur un microbe invisible antagoniste des bactérie dysentériques," *Comptes rendus hebdomadaires des séances de l'Académie des sciences*, vol. 165, p. 373, 1917.

[94] J.-F. Vieu, G. F., M. R., and N. P., "Donneees actuelles sur les applications therapeutiques des bacteriophages," *Bull. Acad.Natl.Med*, vol. 163, p. 61, 1979.

[95] P. A. Barrow and J. S. Soothill, "Bacteriophage therapy and prophylaxis: rediscovery and renewed assessment of the potential," *Trends in Microbiology*, vol. 5, pp. 268–271, 1997.

[96] L. Bruce and J. J. Bull, "Phage therapy revisited: The population biology of a bacterial infection and its treatment with bacteriophage and antibiotics," *The American Naturalist*, vol. 147, pp. 881–898, 1996.

[97] C. Merril, B. Biswas, R. Carlton, N. Jensen, G. Creed, S. Zullo, and S. Adhya, "Long-circulating bacteriophages as antibacterial agents," *Proceedings of the National Academy of Science*, vol. 93, pp. 3188–3192, 1996.

[98] J. S. Soothill, "Treatment of experimental infections of mice with bacteriophages," *Journal of Medical Microbiology*, vol. 37, pp. 258–261, Oct 1992.

[99] J. S. Soothill, "Bacteriophage prevents destruction of skin-grafts by pseudonomas-aeruginosa," *Burns*, vol. 20, pp. 209–211, Jun 1994.

[100] N. Sternberg and R. H. Hoess, "Display of peptides and proteins on the surface of bacteriophage-lambda," *Proceedings of the National Academy of Science*, vol. 92, pp. 1609–1613, Feb 1995.

[101] P. M. G. F. Vanwezenbeek, T. J. M. Hulsebos, and J. G. G. Schoenmakers, "Nucleotide sequence of the filamentous bacteriophage m13 dna genome - comparison with phage fd," *Gene*, vol. 11, no. 1-2, pp. 129–148, 1980.

[102] W. B. Wood and H. R. Revel, "Genome of bacteriophage-t4," *Bacteriological Reviews*, vol. 40, no. 4, pp. 847–868, 1976.

[103] D. J. J. and F. W. Studier, "Complete nucleotide-sequence of bacteriophage-t7 dna and the locations of t7 genetic elements," *Journal of Molecular Biology*, vol. 166, no. 4, pp. 477–535, 1983.

[104] D. F. Hill and G. B. Petersen, "Nucleotide sequence of bacteriophage f1 dna," *Journal of Virology*, vol. 44, no. 1, pp. 32–46, 1982.

[105] E. Kutter and A. Sulakvelidze, *Bacteriophages: Biology and Applications*. CRC Press, Boca Raton, Fl, 2004.

[106] E. Kutter, "www.evergreen.edu/phage," *Evergreen State College, Olympia, Washington*, May 2007.

[107] C. F. Barbas, A. S. Kang, R. A. Lerner, and S. J. Benkovic, "Assembly of combinatorial antibody libraries on phage surfaces - the gene iii site," *Proceedings of the National Academy of Science of the United States of America*, vol. 88, pp. 7978–7982, Sep 1991.

[108] G. Winter, A. D. Griffits, R. E. Hawkins, and H. R. Hoogenboom, "Making antibodies by phage display technology," *Annual Review of Immunology*, vol. 12, pp. 433–455, 1994.

[109] R. Edgar, M. McKinstry, J. Hwang, A. B. Oppenheim, R. A. Fekete, G. Giulian, C. Merril, K. Nagashima, and S. Adhya, "High-sensitivity bacterial detection using biotin-tagged phage and quantum-dot nanocomplexes," *Proceedings of the National Academy of Science of the United States of America*, vol. 103, pp. 4841–4845, Mar 2006.

[110] M. Dobozi-King, S. Seo, J. Kim, R. Young, M. Cheng, and L. Kish, "Rapid detection and identification of bacteria: Sensing of phage-triggered ion cascade (septic)," *Journal of Biological Physics and Chemistry*, vol. 5, pp. 3–7, 2005.

[111] S. Seo, H. C. Kim, M. S. Cheng, X. C. Ruan, and W. Ruan, "Microelectrical noise detector for rapid, specific, and sensitive identification of bacteria," *Journal of Vacuum Science & Technology B*, vol. 24, pp. 3133–3138, Nov-Dec 2006.

[112] V. Nanduri, I. B. Sorokulova, A. M. Samoylov, A. L. Simonian, V. A. Petrenko, and V. Vodyanoy, "Phage as a molecular recognition element in biosensors immobilized by physical adsorption," *Biosensors & Bioelectronics*, vol. 22, pp. 986–992, Jan 2007.

[113] S. Balasubramanian, I. B. Sorokulova, V. J. Vodyanoy, and A. L. Simonian, "Lytic phage as a specific and selective probe for detection of staphylococcus aureus - a surface plasmon resonance spectroscopic study," *Biosensors & Bioelectronics*, vol. 22, pp. 948–955, Jan 2007.

[114] S. Kossek, C. Padeste, and L. Tiefenauer, "Immobilization of streptavidin for immunosensors and nanostructured surfaces," *Journal of Molecular Recognition*, vol. 9, pp. 485–487, 1996.

[115] T. Bran, V. Barwich, M. K. Ghatkesar, A. H. Bredekamp, C. Gerber, M. Hegner, and H. P. Lang, "Micromechanical mass sensors for biomolecular detection in a physiological environment," *Physical Review*, vol. E 72, 2005.

[116] J. J. Gau, E. H. Lan, B. Dunn, C. M. Ho, and J. C. S. Woo, "A mems based amperometric detector for e. coli bacteria using self-assembled monolayers," *Biosensors & Bioelectronics*, vol. E 16, pp. 745–755, 2001.

[117] M. V. Merritt, M. Mrksich, and G. M. Whitesides, "Using self-assembled monolayers to study interactions of man-made materials with proteins," *Principles of tissue engineering*, pp. 211–223, 1997.

[118] M. Mrksich and G. M. Whitesides, "Using self-assembled monolayers to understand the interactions of man-made surfaces with proteins and cell," *Annual Review of Biophysics and Biomolecular Structures*, vol. 25, pp. 55–78, 1996.

[119] N. K. Chaki and K. Vijayamohanan, "Self-assembled monolayers as a tunable platform for biosensor applications," *Biosensors & Bioelectronics*, vol. 17, pp. 1–12, 2001.

[120] A. Ulman, "Formation and structure of self-assembled monolayers," *Chemical Review*, vol. 96, pp. 1533–1554, 1996.

[121] W. Senaratne, L. Andruzzi, and C. K. Ober, "Self-assembled monolayers and polymer brushes in biotechnology: current applications and future perspectives," *Biomacromolecules*, vol. 6, pp. 2427–2448, 2005.

[122] R. Sandberg, K. Molhave, A. Boisen, and W. Svendsen, "Effect of gold coating on the q-factor of a resonant cantilever," *Journal of Micromechanics and Microengineering*, vol. 15, pp. 2249–2253, Dec 2005.

[123] G. M. Whitesides, E. Ostuni, S. Takayama, X. Y. Jiang, and D. E. Ingber, "Soft lithography in biology and biochemistry," *Annual Review of Biomedical Engineering*, vol. 3, pp. 335–373, 2001.

[124] J. J. Gooding, F. Mearns, W. R. Yang, and J. Q. Liu, "Self-assembled monolayers into the 21(st) century: Recent advances and applications," *Electroanalysis*, vol. 15, pp. 81–96, Feb 2003.

[125] F. Schreiber, "Structure and growth of self-assembling monolayers," *Progress in Surface Science*, vol. 65, pp. 151–256, Nov-Dec 2000.

[126] D. S. Ginger, H. Zhang, and C. A. Mirkin, "The evolution of dip-pen nanolithography," *Angewandte Chemie-International Edition*, vol. 43, no. 1, pp. 30–45, 2004.

[127] J. Y. Huang, D. A. Dahlgren, and J. C. Hemminger, "Photopatterning of self-assembled alkanethiolate monolayers on gold - a simple monolayer photoresist utilizing aqueous chemistry," *LANGMUIR*, vol. 10, pp. 626–628, Mar 1994.

[128] R. K. Smith, P. A. Lewis, and P. S. Weiss, "Patterning self-assembled monolayers," *Progress in Surface Science*, vol. 75, pp. 1–68, Jun 2004.

[129] R. S. Kane, S. Takayama, E. Ostuni, D. E. Ingber, and G. M. Whitesides, "Patterning proteins and cells using soft lithography," *Biomaterials*, vol. 20, pp. 2363–2376, Dec 1999.

[130] M. Boncheva, D. A. Bruzewicz, and G. M. Whitesides, "Millimeter-scale self-assembly and its applications," *Pure and Applied Chemistry*, vol. 75, pp. 621–630, May 2003.

[131] J. Voldman, M. L. Gray, and M. A. Schmidt, "Microfabrication in biology and medicine," *Annual Review of Biomedical Engineering*, vol. 1, pp. 401–425, 1999.

[132] M. e. a. Savage, *Avidin-Biotin Chemistry: A Handbook*, vol. xxvii. Pierce Chemical Company, 2nd ed., 1994.

[133] W. Ganong, *Review of medical physiology*. Norwalk, Connecticut: Appleton & Lange, 13th ed., 1987.

[134] E. P. Diamandis and T. K. Christopoulos, "The biotin(streptavidin) system - principles and applications in biotechnology," *Clinical Chemistry*, vol. 37, pp. 625–636, May 1991.

[135] P. Vermette, T. Gengenbach, U. Divisekera, P. A. Kambouris, H. J. Griesser, and L. Meagher, "Immobilization and surface characterization of neutravidin biotin-binding protein on different hydrogel interlayers," *Journal of Coloid and Interface Science*, vol. 259, pp. 13–26, Mar 2003.

[136] C. M. Pradier, M. Salmain, Z. Liu, and C. Methivier, "Comparison of different procedures of biotin immobilization on gold for the molecular recognition of avidin: an ft-irras study," *Surface and Interface Analysis*, vol. 34, pp. 67–71, Aug 2002.

[137] M. Riepl, K. Enander, B. Liedberg, M. Schaferling, M. Kruschina, and F. Ortigao, "Functionalized surfaces of mixed alkanethiols on gold as a platform for oligonucleotide microarrays," *Langmuir*, vol. 18, pp. 7016–7023, Sep 2002.

[138] J. S. Shumaker-Parry, M. H. Zareie, R. Aebersold, and C. T. Campbell, "Microspotting streptavidin and double-stranded dna arrays on gold for high-throughput studies of protein-dna interactions by surface plasmon resonance microscopy," *Analytical Chemistry*, vol. 76, pp. 918–929, Feb 2004.

[139] J. Spinke, M. Liley, F. J. Schmitt, H. J. Guder, L. Angermaier, and W. Knoll, "Molecular recognition at self-assembled monolayers - optimization of surface functionalization," *Journal of Chemical Physics*, vol. 99, pp. 7012–7019, Nov 1993.

[140] W. Sun, L. Brovko, and M. Griffiths, "Use of bioluminescent salmonella for assessing the efficiency of constructed phage-based biosorbent," *Journal of Industrial Microbiology and Biotechnology*, vol. 27, p. 126, 2001.

[141] M. Tolba, L. Brovko, and M. Griffiths *unreported*, 2006.

[142] F. Ligler, C. Taitt, L. Shriver-Lake, K. Sapsford, Y. Shubin, and J. Golden, "Array biosensor for detection of toxins," *Anal. Bioanal. Chem.*, vol. 377, pp. 469–477, 2003.

[143] N. Kulagina, M. Lassman, F. Ligler, and C. Taitt, "Antimicrobial peptides for detection of bacteria in biosensor assays," *Anal. Chem.*, vol. 77, pp. 6504–6508, 2005.

[144] K. Heller, "Molecular interaction between bacteriophage and the gram-negative cell envelope," *Arch Microbiol*, vol. 158, no. 4, pp. 235–248, 1992.

[145] J. Wilson and R. L. W. Wood, "Interaction of bacteriophage t4 tail fiber components with a lipopolysaccharide fraction from escherichia coli," *Journal of Molecular Biology*, vol. 51, no. 423-434, 1970.

[146] D. Montag, H. Schwarz, and U. Henning, "A component of the side tail fiber of escherichia coli bacteriophage lambda can functionally replace the receptor-recognizing part of a long tail fiber protein of the unrelated bacteriophage t4," *Journal of Bacteriology*, vol. 171, no. 8, pp. 4378–4384, 1989.

[147] G. Olsen, C. Woese, and R. Overbeek, "The winds of (evolutionary) change: breathing new life into microbiology," *Journal of Bacteriology*, vol. 176, no. 1, pp. 1–6, 1994.

[148] H. Ochman and A. Wilson, "Evolution in bacteria: evidence for a universal substitution rate in cellular genomes," *Mol. Evol.*, vol. 26, no. 1-2, pp. 74–86, 1987.

[149] J. Sambrook and D. W. R. et al., *Molecular cloning: A laboratory manual.* Cold Spring Harbor, New-York: Cold Spring Harbor Laboratory Press, 2nd edition ed., 1989.

[150] G. S. Huang, M. T. Wang, and M. Y. Hong, "A versatile qcm matrix system for online and high-throughput bio-sensing," *Analyst*, vol. 131, pp. 382–387, 2006.

[151] D. Ivnitski, I. Abdel-Hamid, P. Atanasov, and E. Wilkins, "Biosensors for detection of pathogenic bacteria," *Biosensors & Bioelectronics*, vol. 14, pp. 599–624, Oct 1999.

[152] S. Lan, M. Veiseh, and M. Q. Zhang, "Surface modification of silicon and gold-patterned silicon surfaces for improved biocompatibility and cell patterning selectivity," *Biosensors & Bioelectronics*, vol. 20, pp. 1697–1708, Mar 2005.

[153] B. D. Ratner and S. J. Bryant, "Biomaterials: Where we have been and where we are going," *Annual Review of Biomedical Engineering*, vol. 6, pp. 41–75, 2004.

[154] A. C. R. Grayson, R. S. Shawgo, A. M. Johnson, N. T. Flynn, Y. W. Li, M. J. Cima, and R. Langer, "A biomems review: Mems technology for physiologically integrated devices," *Proceeding of the IEEE*, vol. 92, pp. 6–21, Jan 2004.

[155] D. J. Beebe, G. A. Mensing, and G. M. Walker, "Physics and applications of microfluidics in biology," *Annual Review of Biomedical Engineering*, vol. 4, pp. 261–286, 2002.

[156] D. L. Polla, A. G. Erdman, W. P. Robbins, D. T. Markus, J. Diaz-Diaz, R. Rizq, Y. Nam, H. T. Brickner, A. Wang, and P. Krulevitch, "Microdevices in medicine," *Annual Review of Biomedical Engineering*, vol. 2, pp. 551–576, 2000.

[157] E. Uttenthaler, M. Schraml, J. Mandel, and S. Drost, "Ultrasensitive quartz crystal microbalance sensors for detection of m13-phages in liquids," *Biosensors & Bioelectronics*, vol. 16, pp. 735–743, Dec 2001.

[158] O. Tamarm, S. Comeau, C. Dejous, D. Moynet, D. Rebiere, J. Bezian, and J. Pistre, "Real time device for biosensing: design of a bacteriophage model using love acoustic waves," *Biosensors & Bioelectronics*, vol. 18, pp. 755–763, May 2003.

[159] L. B. Kish, M. Cheng, J. U. Kim, S. Seo, M. D. King, R. Young, A. Der, and G. Schmera, "Estimation of detection limits of the phage-invasion based identification of bacteria," *Fluctuation and Noise Letters*, vol. 5, pp. L105–L108, Mar 2005.

[160] N. L. Rosi and C. A. Mirkin, "Nanostructures in biodiagnostics," *Chemical Review*, vol. 105, pp. 1547–1562, Apr 2005.

[161] S. Bhattacharya, J. S. Jang, L. J. Yang, D. Akin, and R. Bashir, "Biomems and nanotechnology-based approaches for rapid detection of biological entities," *Journal of Rapid Methods and Automation in Microbiology*, vol. 15, pp. 1–32, Mar 2007.

[162] A. D. Hershey, "Reproduction of bacteriophages," *International review of cytology-a survey of cell biology*, vol. 1, pp. 119–134, 1952.

[163] T. Wink, S. J. V. Zuilen, A. Bult, and W. P. V. Bennekom, "Self-assembled monolayers for biosensors," *Analyst*, vol. 122, pp. 43R–50R, 1997.